Comparative Investigation of Ruthenium-Based Metathesis Catalysts Bearing N-Heterocyclic Carbene (NHC) Ligands

Alois Fürstner,* Lutz Ackermann, Barbara Gabor, Richard Goddard, Christian W. Lehmann, Richard Mynott, Frank Stelzer, and Oliver R. Thiel[a]

Abstract: Exchange of one PCy_3 unit of the classical Grubbs catalyst **1** by N-heterocyclic carbene (NHC) ligands leads to "second-generation" metathesis catalysts of superior reactivity and increased stability. Several complexes of this type have been prepared and fully characterized, six of them by X-ray crystallography. These include the unique chelate complexes **13** and **14** in which the NHC- and the Ru=CR entities are tethered to form a metallacycle. A particularly favorable design feature is that the reactivity of such catalysts can be easily adjusted by changing the electronic and steric properties of the NHC ligands. The catalytic activity also strongly depends on the solvent used; NMR investigations provide a tentative explanation of this effect. Applications of the "second-generation" catalysts to ring closing alkene metathesis and intramolecular enyne cycloisomerization reactions provide insights into their catalytic performance. From these comparative studies it is deduced that no single catalyst is optimal for different types of applications. The search for the most reactive catalyst for a specific transformation is facilitated by IR thermography allowing a rapid and semi-quantitative ranking among a given set of catalysts.

Keywords: carbenes · imidazol-2-ylidenes · IR thermography · metathesis · ruthenium

Introduction

The seminal discovery of Grubbs that ruthenium carbene complexes of type **1** constitute well defined and highly efficient metathesis pre-catalysts tolerating an array of functional groups has triggered an avalanche of interest in this transformation.[1, 2] This groundbreaking development has inspired many studies aiming at improving access to these exceedingly useful reagents,[3] at gaining a deeper understanding of their mechanism of action,[4] at developing equipotent alternatives,[5] and at designing catalysts with an even better application profile.[6] In this context it is notable that three independent and almost simultaneous publications on "second-generation" metathesis catalysts report complexes in which *one* of the PCy_3 groups of **1** is replaced by an N-heterocyclic carbene (NHC).[7–9] NHCs are particularly strong σ-donor- but very poor π-acceptor ligands which show little tendency to dissociate from the metal center.[10] Since they can be easily endowed with sterically demanding substituents on their N-atoms, they are able to stabilize the catalytically relevant intermediates by electronic and steric means against uni- as well as bimolecular decomposition pathways. These properties translate into catalysts of greatly improved reactivity as well as higher stability which outperform the parent-complex **1** in many cases. Successful applications to the formation of tetrasubstituted cycloalkenes,[8, 9] to ring closing- and cross metathesis reactions of acrylates,[11, 12] to cyclizations of conformationally handicapped dienes and various natural product syntheses highlight this notion.[13, 14] Therefore, it is reasonable to anticipate that NHC-containing ruthenium complexes will set new standards in this still rapidly expanding field.

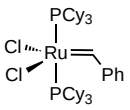

1

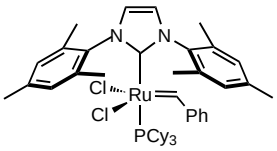

2

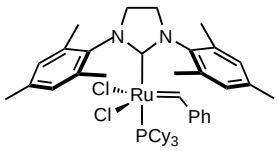

3

The studies on NHC-containing catalysts reported so far, however, gravitate toward complexes **2** and **3** bearing identical substituents on both N-atoms of their saturated or unsaturated NHC rings.[15] Herein we report a more compre-

[a] Prof. Dr. A. Fürstner, Dipl.-Chem. L. Ackermann, B. Gabor, Dr. R. Goddard, Dr. C. W. Lehmann, Dr. R. Mynott, Dipl.-Chem. F. Stelzer, Dipl.-Chem. O. R. Thiel
Max-Planck-Institut für Kohlenforschung
45470 Mülheim/Ruhr (Germany)
Fax: (+49) 208-306-2994
E-mail: fuerstner@mpi-muelheim.mpg.de

0947-6539/01/0715-3236 $ 17.50+.50/0

hensive investigation on the preparation, structure, and reactivity of such "second-generation" metathesis catalysts including complexes with symmetrically or *unsymmetrically* substituted NHC entities, as well as with *chelating* carbene ligands, respectively. It will be demonstrated that the resulting pool of catalysts can be assessed in parallel by IR thermography, thus enabling a rapid selection of the optimal catalyst(s) for a given transformation. Finally, preparative applications to a representative set of metathesis reactions and a detailed study on enyne metathesis provide insights into the specificities of these powerful new tools.

Results and Discussion

Preparation of the catalysts: Although the synthesis of the required imidazolium salts,[16] the N-heterocyclic carbenes derived thereof,[16–18] and the ruthenium complexes[7–9] is straightforward when following literature routes, some comments are necessary. The symmetrical imidazolium salts **4** (Scheme 1) are obtained by condensation of the corresponding amine, glyoxal and a C-1 synthon (paraformaldehyde, $HC(OEt)_3$ or $ClCH_2OEt$) as previously described,[16–18] whereas the unsymmetrically substituted derivatives **7** (Scheme 2) used in this study are prepared by quarternization of *N*-mesitylimidazole (**6**).[19]

Deprotonation of **4** with *t*BuOK[20] in THF affords the corresponding free carbenes **5** which can be isolated and stored at low temperature under Ar for several weeks (Schemes 1 and 2). The chloro-substituted carbene **5c** is obtained on treatment of **5a** with CCl_4 as outlined by Arduengo et al.[17a]

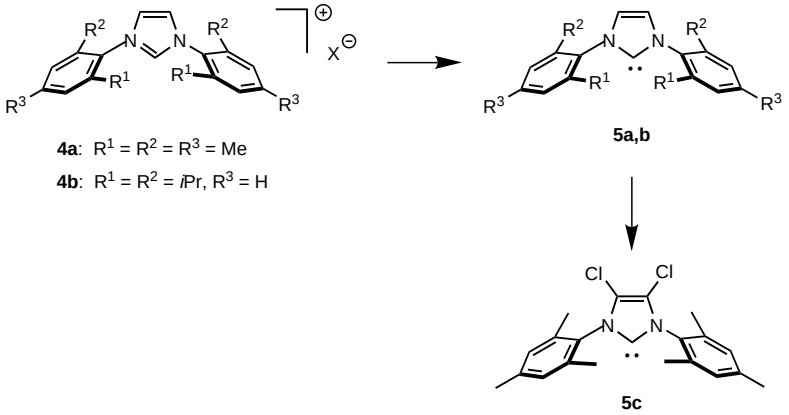

Scheme 1.

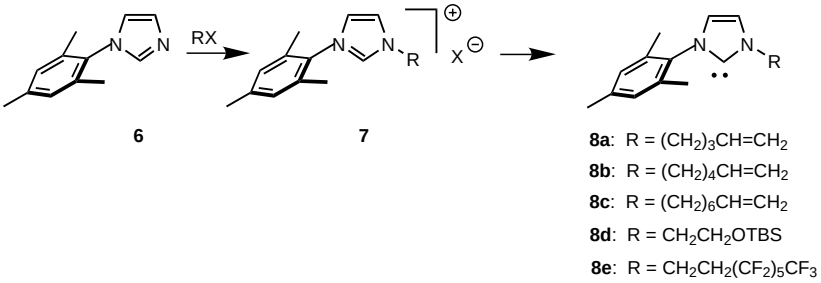

Scheme 2.

Exposure of the parent Grubbs complex **1** to one of the N-heterocyclic carbenes **5a–c** (1.1–1.3 equiv) in toluene at ambient temperature affords the desired catalysts (Scheme 3).[7–9] Only in the case of the more sterically

Scheme 3.

hindered derivative **10** must the reaction be carried out at 50 °C to ensure a reasonable rate. In most cases, the replacement of one PCy_3 unit of **1** by the NHC can be conveniently monitored by TLC using *n*-hexane/ethyl acetate (4:1) as the eluent. Complexes **2**, **9**, and **10** thus formed can either be purified by repeated washing with pentane, or, preferentially, by routine flash chromatography on silica gel. They are thermally stable, rather inert towards oxygen and moisture, and can be stored for extended periods of time without any appreciable loss of reactivity.

The preparation of complex **11** follows the same route and is particularly straightforward since the required ligand, that is 1,3,4-triphenyl-4,5-dihydro-1*H*-1,2,4-triazol-5-ylidene,[21] is commercially available. Reaction with the Grubbs catalyst **1** in toluene at ambient temperature furnishes the desired substitution product **11** in 72% yield. In crystalline form this compound can be stored under Ar for several weeks, but when kept in chlorinated solvents it decomposes rapidly to as yet unidentified products. The significantly lower stability of **11** in solution as compared to the other members of this series is a limiting factor for its preparative utility (see below).

It is important to note that the procedure described above involving the *isolation* of the free N-heterocyclic carbenes as a separate step is generally preferred over a more user-friendly "in situ" method recently outlined in the literature in which all ingredients, that is the imidazolium salt, complex **1** and *t*BuOK, are mixed together and reacted in *n*-hexane.[22] For example, if applied to the synthesis of **10** this one-pot procedure produces significant amounts of by-products thus making the isolation of the desired complex quite difficult. According to IR and NMR spectroscopic data, at least one of the contaminants is a ruthenium hydride species which may be responsible for side reactions (see below). Despite of this inconvenience, the "in situ" protocol was chosen to prepare the olefinic complexes **12a–c** in order to minimize possible side reactions between the carbene center and the alkene groups in the lateral chains of the NHC derivatives **8a–c** formed from **7a–c** and *t*BuOK.[21b]

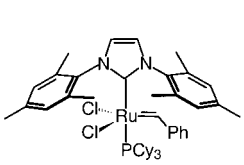

2

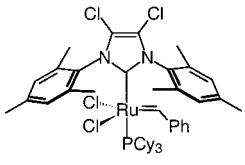

9

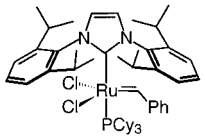

10

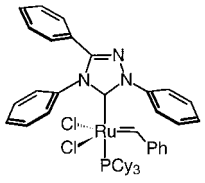

11

The unique ability of complexes **12a–c** to *metathesize their own ligands* lays the ground for the preparation of compounds **13** and **14** in which the N-heterocyclic carbene and the "regular" carbene unit Ru=CHR are tethered to form a metallacycle. Specifically, heating a solution of complex **12b** in refluxing pentane or toluene (80 °C) affords chelate **13** in 75% isolated yield; the course of the reaction can again be monitored by TLC. The shorter homologue **14** is prepared analogously starting from complex **12a** as the precursor. The design of these species is based on the idea that they might be able to regenerate themselves after the productive metathesis is over and the substrate in solution has been quantitatively consumed.

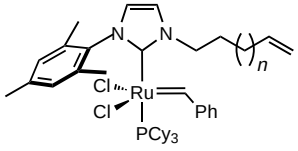

12a: $n = 1$
12b: $n = 2$
12c: $n = 4$

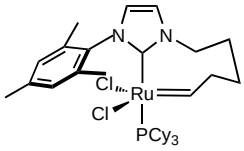

13

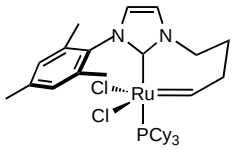

14

Additional unsymmetrically substituted NHC complexes displaying further structural variations are the silylether derivative **15** and complex **16** incorporating a perfluoroalkyl chain.[23]

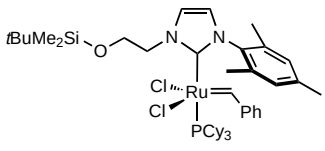

15

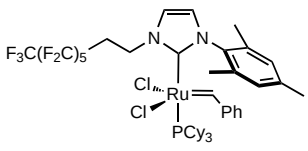

16

Structure: The crystal structures of **9**, **10**, **11**, **13**, **14**, and **15** have been determined (Figure 1–6), and allow us to look for

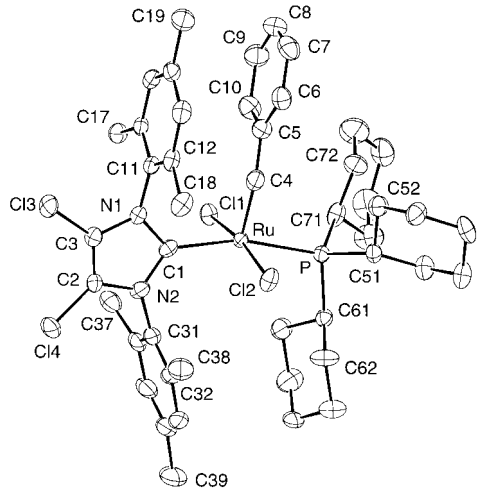

Figure 1. Molecular structure of complex **9**, anisotropic displacement parameters are drawn at 50% probability, hydrogen atoms omitted for clarity.

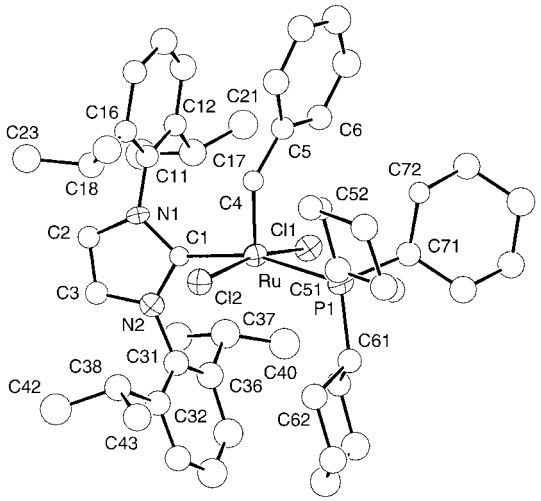

Figure 2. Molecular structure of complex **10**, anisotropic displacement parameters are drawn at 50% probability, hydrogen atoms omitted for clarity.

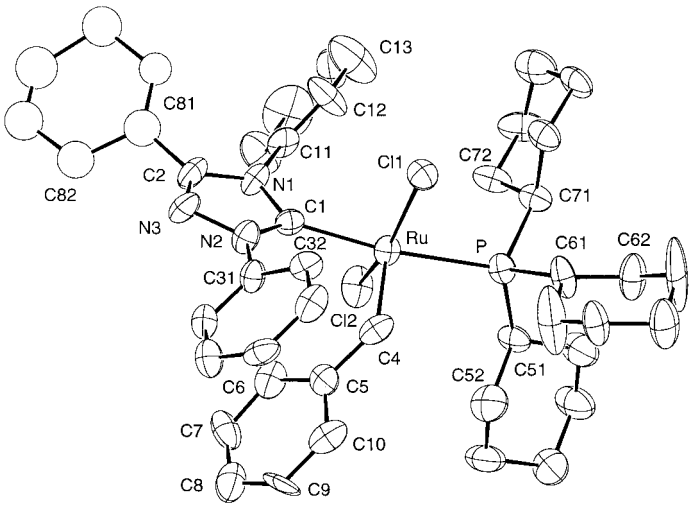

Figure 3. Molecular structure of complex **11**, anisotropic displacement parameters are drawn at 50% probability, hydrogen atoms omitted for clarity.

0947-6539/01/0715-3238 $ 17.50+.50/0 *Chem. Eur. J.* **2001**, *7*, No. 15

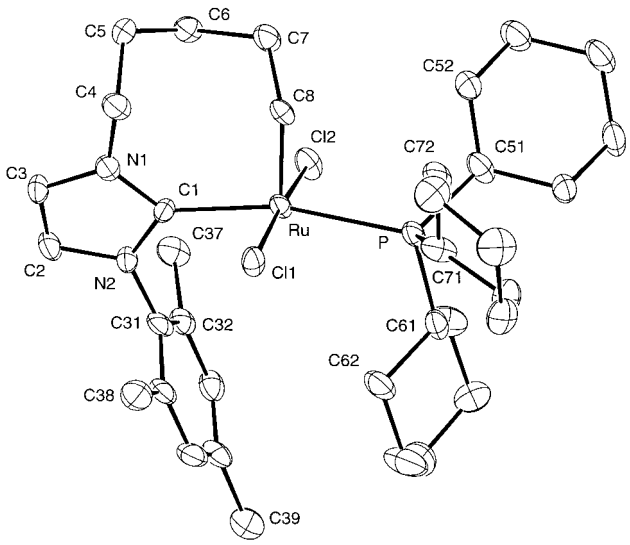

Figure 4. Molecular structure of complex **13**, anisotropic displacement parameters are drawn at 50% probability, hydrogen atoms omitted for clarity.

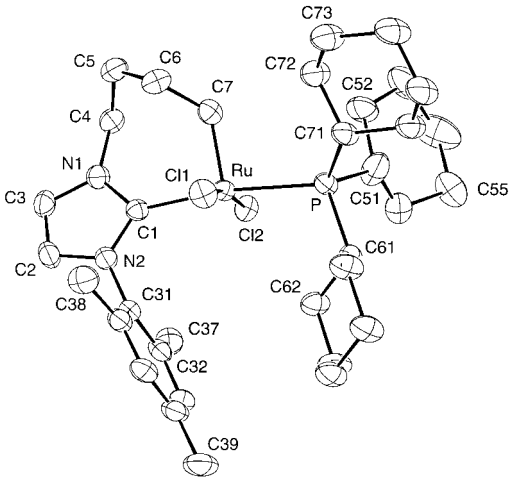

Figure 5. Molecular structure of complex **14**, anisotropic displacement parameters are drawn at 50% probability, hydrogen atoms omitted for clarity.

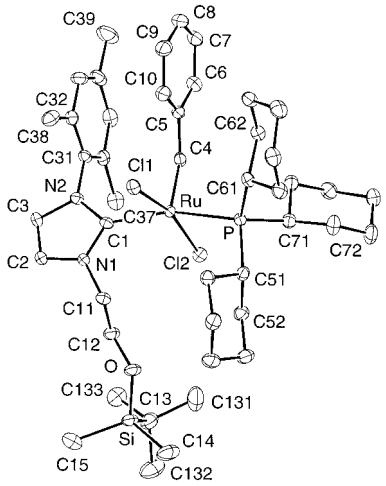

Figure 6. Molecular structure of complex **15**, anisotropic displacement parameters are drawn at 50% probability, hydrogen atoms omitted for clarity.

correlations between the catalytic activity and structural properties of this class of compounds. Two related structures published by others (i.e., X-ray structures of complex **2**[7a] and a polymorph of complex **10**[15c]) have been included to extend the basis of this comparison.

In all structures the Ru^{II} center is pentacoordinate; its geometry lies between the idealized forms of a trigonal bipyramid and a square pyramid and is closer to the latter. In all cases the two chlorine ligands are *trans*-oriented in the basal plane of the square pyramid, with the phosphorus atoms and the imidazolyl carbene carbon atom occupying the remaining corners. The benzylidene carbene ligand always occupies the apical position.

A number of interatomic bond and contact parameters have been extracted from the structures for a more detailed comparison. These parameters are the averaged Ru-ligand distances, the Cl-Ru-Cl bond angle, the P-Ru-imidazolyl bond angle, the rms deviation of these four ligands from a least-squares plane, and the distance of the Ru atom from this plane (Table 1). The dihedral angle between the Cl-Ru-Cl and the carbene double bond (Ru=CPh) is also given. A dihedral angle of 0° corresponds to an orientation in which the π orbitals are perpendicular to the Cl-Ru-Cl plane.

The overall geometries of **9**, **10**, **11**, **13**, **14**, and **15** are surprisingly similar in the sense that all PCy_3 ligands adopt approximately the same conformation with respect to the Ru–P bond. The NHC ligand is always co-planar with the carbene and in the case of asymmetrically substituted NHCs (**11**, **13**, **14**, and **15**) no rotamer disorder around the C–Ru bond has been observed in the crystal.[24] While the tethered carbenes **13** and **14** force the mesitylene group to the side of the chlorines (Figure 4 and 5), the mesitylene group in **15** is oriented towards the benzylidene (Figure 6). The distance between the mesitylene and the benzylidene ring is 3.44 Å and both rings are co-planar within 7.9°. This π–π interaction is preserved to some extent in solution (see below) and can also be observed in the triazol complex **11** (Figure 3), although in this case the benzylidene adopts a rather different orientation as can be seen from Table 1. The angle between the *N*-phenyl and the benzylidene ring is 14.0° and the distance between the two rings is 3.31 Å. Similar π–π interactions are found in the other molecules (with the exception of the polymorph of **10c** reported by Nolan) and are all well within the range observed for aromatic stacking.[25] Although the observed preservation of molecular conformational detail throughout the range of compounds studied suggests only a small influence of crystal packing, two points must be noted. In the crystal structure of **11** the phenyl ring attached to C2 in the triazol is disordered (Figure 3), which might explain the different orientation of the benzylidene.

Secondly and more importantly Nolan et al. report for **10** a different polymorph (i.e., **10c**)[15c] with rather different molecular shape. A closer inspection of the crystal packing of **10a,b** prepared in our laboratory reveals Cl···H contacts of 2.7 and 2.8 Å between Cl2 and H2 (one of the hydrogen atoms in the imidazolyl ring) linked through a 2_1 screw-axis in both independent molecules. In contrast, structure **10c** does not feature this interaction.[15c] If viewed along the crystallo-

Table 1. Selected bond parameters of the Ru^{II} coordination sphere for **9**, **10a**,**b**, **11**, **13**, **14**, **15** and the previously reported **2**[7a] and **10c**.[15c]

Compound	**11**	**10a**	**10b**	**10c**[15c]	**9**	**2**[7a]	**15**	**13**	**14**
< Ru−Cl >	2.349(3)	2.373(4)	2.373(4)	2.3914(7)	2.3876(11)	2.388(3)	2.4581(5)[d]	2.3973(16)	2.3848(8)
Ru−P	2.440(3)	2.390(4)	2.381(4)	2.4554(1)	2.4160(12)	2.419(3)	2.4231(7)	2.4214(17)	2.4020(8)
Ru−C	2.085(9)	2.049(12)	2.067(8)	2.088(2)	2.092(5)	2.069(11)	2.056(3)	2.091(6)	2.076(3)
Ru=C	1.819(10)	1.795(11)	1.840(13)	1.817(3)	1.846(5)	1.841(11)	1.835(3)	1.806(6)	1.812(3)
Cl-Ru-Cl	156.94(10)	168.75(13)	168.04(15)	170.42(2)	169.43(4)	168.62(12)	165.240(18)	174.14(6)	168.20(3)
C-Ru-P	171.8(3)	164.0(4)	162.1(3)	164.60(1)	163.89(12)	163.2(3)	161.91(7)	165.99(18)	170.98(8)
α [°][a]	46.0	15.4	17.4	38.7	15.0	18.0	16.5	26.6	51.3
d[b] [Å]	0.32	0.26	0.29	0.23	0.26	0.28	0.33	0.08	0.21
planarity[c]	0.15	0.04	0.05	0.06	0.05	0.04	0.02	0.04	0.03

[a] Dihedral angle between the planes Cl-Ru-Cl and C−C=Ru. [b] Distance of the Ru atom from the least-squares plane formed by the two chlorine atoms, P and the imidazolyl carbene carbon atom. [c] Root-mean-square deviation of the four atoms under [b] from the least-squares-plane. [d] The unexpectedly long averaged Ru−Cl bond is due to the fact that 19% of Cl1 and 35% of Cl2 are disordered with Br.

graphic *b* axis the differences between the two polymorphic forms of **10a**,**b** are most prominent. In the polymorph **10c** reported by Nolan the molecules form clearly separated stacks along the *b* direction. Molecules related by symmetry interact with these stacks by intersecting one cyclohexyl ring, employing a 2_1 screw-axis passing through the ring (Figure 7). In **10a**,**b** prepared in our laboratory a completely different picture is seen. Viewed along the *b* axis (which is almost 1.5 times as long as in **10c**) the two independent molecules arrange in a one-up/one-down fashion, with a large degree of overlap (Figure 8). This results in a zig-zag chain along the *b* direction which is held together by the H···Cl interactions described above. The crystal packing also reveals the formation of two channels parallel to the *b* axis. A larger diameter one is centered at $x = 0.5$, $z = 0.5$, and a smaller one at $x = 0$, $z = 0$. Those channels are filled with disordered solvent molecules (pentane).

The superposition of these three molecules of **10a**–**c** shown in Figure 9 compared with the superposition of the six remaining ruthenium(II) carbenes (Figure 10) reveals the

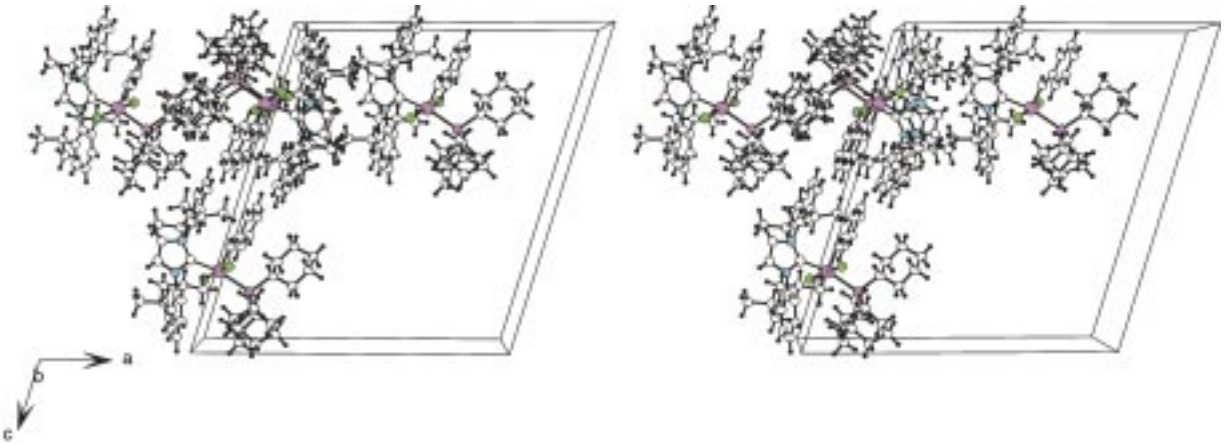

Figure 7. Stereoview of the crystal packing of complex **10c** viewed along the *b* axis, *c* axis vertical.

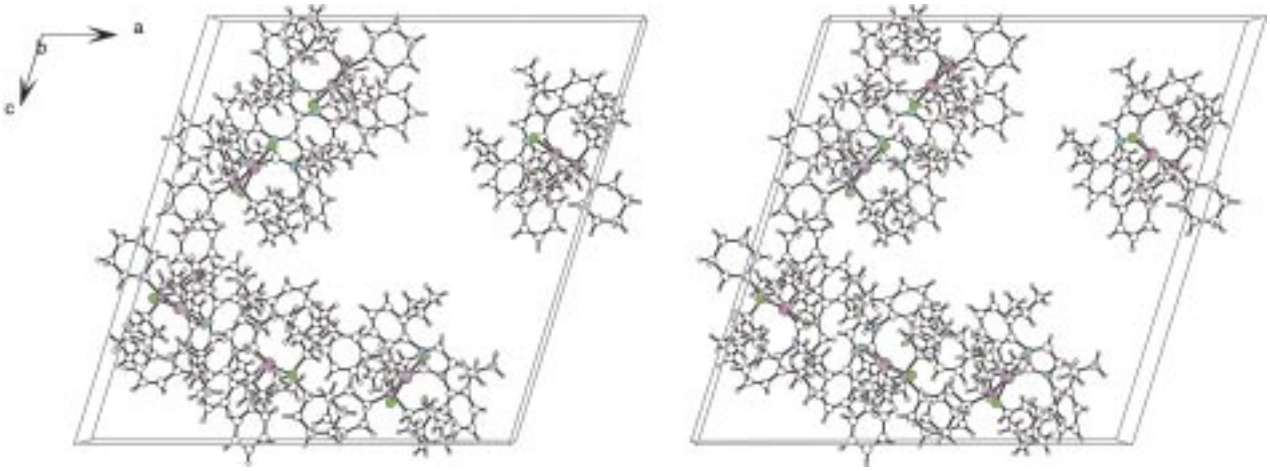

Figure 8. Stereoview of the crystal packing of complex **10a**,**b** viewed along the *b* axis, *c* axis vertical.

0947-6539/01/0715-3240 $ 17.50+.50/0 *Chem. Eur. J.* **2001**, *7*, No. 15

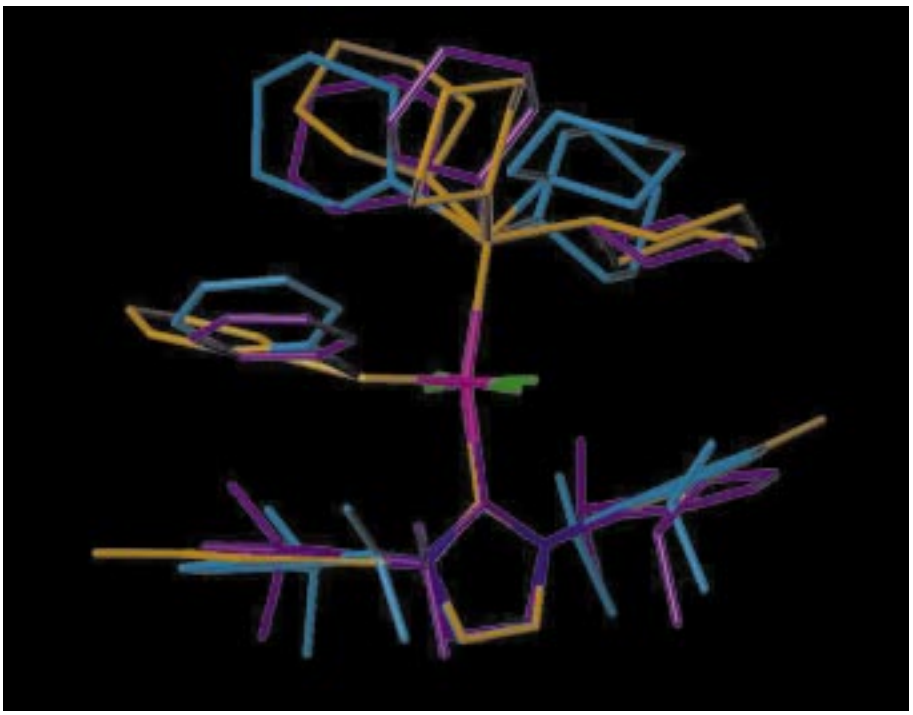

Figure 9. Superposition of the polymorphs of complex **10** using the following color code: **10a** (cyan), **10b** (mauve), **10c**[15c] (orange).

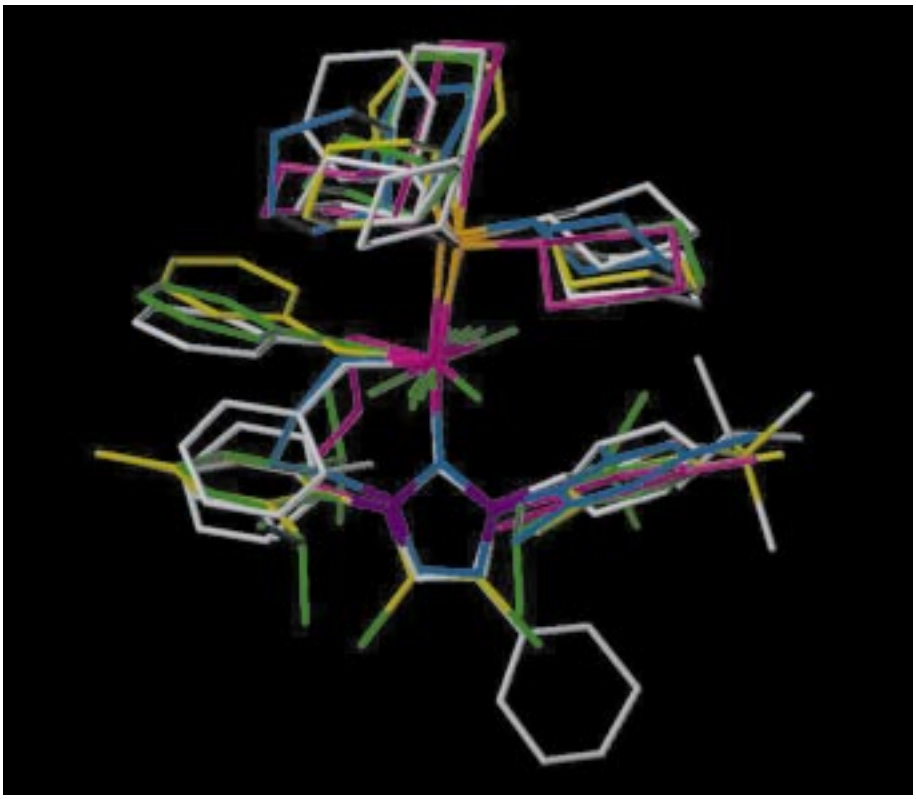

Figure 10. Superposition of "second-generation" metathesis catalysts bearing NHC ligands. Color code: Complex **9** (yellow), complex **10** (green), complex **11** (white), complex **13** (magenta), complex **14** (cyan), complex **15** (white).

unusual orientation of the PCy_3. All cyclohexyl rings in the polymorph **10c** reported by Nolan are rotated and the ring oriented *gauche* to the two chlorine atoms now adopts a conformation where the ring plane is parallel to the Ru–P axis. In all the other molecules of this series, this ring plane is perpendicular. This observation is in agreement with the larger Cl-Ru-Cl bond angle and the longer Ru–Cl bond distances, compared with **10a** and **10b**. It cannot be ruled out that the different molecular conformation of **10c** results from the more dense packing ($\rho =$ 1.279 $Mg\,m^{-3}$) compared with the polymorph of **10a**,**b** prepared in Mülheim ($\rho =$ 1.179 $Mg\,m^{-3}$).

A direct correlation between the benzylidene–Ru bond distance or the dihedral angle between the double bond and the Cl-Ru-Cl plane and any other geometrical parameter is not given. This leads to the conclusion that more complex electronic interactions, in particular the nature of the NHC ligand and the "regular" carbene ligand, are responsible for the geometric interactions. This is in agreement with the more trigonal bipyramidal geometry of the triazolyl complex **11** (Figure 3) which is not present in the other molecules. At the other end of the series is the chelate complex **13** where the carbene lacks the possibility of delocalizing the metal–carbon bond into the phenyl ring (Figure 4). Complex **13** is also the representative which resembles most closely octahedral geometry, with the Ru atom in the plane of the two chlorines, the phosphorus atom and the imidazolyl carbon atom. The closely related chelate complex **14**, which has a four carbon bridge instead of five carbon atoms in **13**, adopts a geometry reflecting the steric strain caused by the shorter tether. Hence, the carbene bond is rotated by 51.3° out of the Cl-Ru-Cl plane and the NHC ligand is twisted by 24° out of the C1-Ru-C7 plane (Figure 5).

Finally, it is worth mentioning that the substitution of the hydrogens of C4 and C5 of the imidazol ring with chlorine in **9** appears to have no effect on the geometry of the molecule. Thus, the structure of complex **9** in the solid (Figure 1) and

that of the unsubstituted complex **2** reported by Nolan[7a] are virtually identical.

NMR investigations—Possible explanation for the pronounced solvent dependence of the catalytic activity of complex 2: The X-ray structures discussed above suggest that the $\pi-\pi$ stacking between the benzylidene carbene unit and the N-aryl substituents on the NHC residues constitutes a strongly conserved structural element in all the second-generation metathesis catalysts described herein. It is of interest to see if this electronic interaction is also operative in solution because it may affect the reactivity of the benzylidene carbene which, in turn, determines the rate of initiation of a metathesis reaction.

Careful analysis of the NMR spectra of complex **2** in CD_2Cl_2 confirm that the rotation of the NHC ligand around the C–Ru bond is restricted, as has already been reported.[24, 26] More importantly, however, the spectra also reveal that the *rotation* of the mesityl substituents around the C–N bond is *hindered*. Two broadened signals are observed in the 600 MHz ^{1}H NMR spectrum of the mesityl protons in CD_2Cl_2. When the spectra are recorded in C_6D_6, however, these signals have coalesced, thus showing that the barrier is lower. Line shape analysis allows one to estimate that the exchange rate is $\approx 480\ s^{-1}$ in CD_2Cl_2 whereas it is $\approx 2000\ s^{-1}$ in C_6D_6, corresponding to an enthalpy difference for the rotational barrier of $\approx 3.5 \pm 0.4\ kJ\,mol^{-1}$ at 300 K.

Competing interactions of the *N*-mesityl group with the aromatic solvent molecules will reduce the stabilizing effect of the intramolecular $\pi-\pi$ stacking with the benzylidene substituent and therefore account for the observed greater conformational freedom. It is tempting to assume that this effect explains

i) why complex **2** is much more reactive in toluene than in CH_2Cl_2 or $ClCH_2CH_2Cl$ solution,[28a]
ii) why this positive influence of toluene is observed only for complexes bearing N-aryl substituents, whereas the activity of analogues with N-alkyl groups on their NHC ligands is usually higher in chlorinated media,[9a] and
iii) why the effect is more pronounced in complex **2** than in complex **10** in which the motion of the larger isopropyl residues on the arene disturb the stabilizing $\pi-\pi$ stacking as can be deduced from a lower rotational barrier around the C–N bond.

Complexes with "saturated" NHC ligands and the isolation of a hydridic by-product: In order to provide a more comprehensive picture, we have also prepared complexes **3**[8b] and **17** bearing "saturated" NHC units and have compared their catalytic performance with that of their "unsaturated" congeners **2** and **10**, respectively. It has recently been claimed that "saturated" NHCs endow the metal center with an even higher reactivity.[8b, 27]

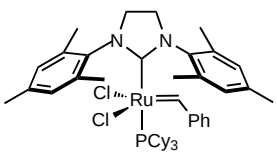

3

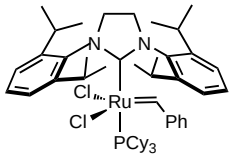

17

Their synthesis was achieved according to the method outlined by Grubbs et al.[8b] through α-elimination of the corresponding 2-*tert*-butoxy-4,5-dihydroimidazole precursors. This procedure works as described for compound **3**; we noticed, however, that increased steric bulk of the N-substituents leads to a deviation from the regular reaction pathway and results in the formation of a hydridic by-product in addition to the desired complex **17** (Scheme 4). A by-product was obtained in pure form by crystallization and was identified as $(PCy_3)_2Ru(H)_2Cl_2$ (**18**). Although we could not directly localize the hydrogen atoms in the X-ray structure of this complex (see below), an absorption band in the IR spectrum ($\tilde{\nu} = 1906\ cm^{-1}$) and a characteristic high field signal in the ^{1}H NMR spectrum ($\delta = -24.38$) unequivocally indicate the presence of hydride ligands. The formation of this species under conditions used for the preparation of catalyst **17** may explain why in some cases the isomerization of the olefinic double bonds of the substrate can compete with productive RCM.[28] This undesirable pathway is likely to be caused by small amounts of metal hydride species formed by decomposition of or by impurities in the metathesis catalysts.

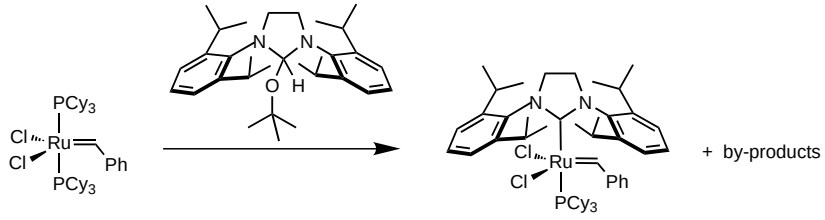

1 **17**

Scheme 4.

***cis*–*trans* Stereoisomerism in $(PCy_3)_2Ru(H)_2Cl_2$**: The molecular structure of **18** (Figure 11) reveals an *octahedral* geometry with a *trans* arrangement of the phosphine groups. The ruthenium atom is situated on a crystallographic inversion center. The presence of two hydrogen atoms in the complex that could not be located in difference Fourier maps has been deduced from spectroscopic data (see above). Complex **18** is the second known crystal structure of a dihydro-dichloro-bis(phosphine)-ruthenium(IV) complex. The first example, $(PiPr_3)_2Ru(H)_2Cl_2$ (**19**) described by Werner et al.,[29] however, is a *distorted square antiprism*. Chaudret et al.[30] report spectroscopic data and theoretical results for the analogous tricyclohexylphosphine complex $(PCy_3)_2Ru(H)_2Cl_2$ (**20**)—a compound having the same composition as complex **18** described herein—which are in agreement with the molecular point group symmetry of **19**.

0947-6539/01/0715-3242 $ 17.50+.50/0 *Chem. Eur. J.* **2001**, *7*, No. 15

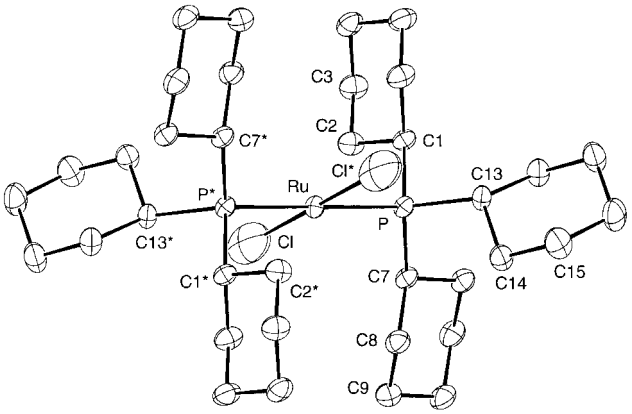

Figure 11. Molecular structure of complex **18**, anisotropic displacement parameters are drawn at 50% probability, hydrogen atoms omitted for clarity.

While the steric requirements of the two different phosphine groups in **18** and **19** are certainly substantially different, this does not explain the different geometries of the two complexes. The formation of **18** by a yet unknown mechanism starts from square pyramidal **1** and thereby leads to the *trans*-octahedral complex.[31] Complexes **19** and **20** on the other hand are formed from $CHCl_3$ and $Ru(H_2)_2(H)_2(PR_3)_2$, a precursor which has already the co-ordinated hydrogen molecule in place to yield the *cis*-geometry of the resulting products. These entirely different syntheses routes may explain why the hydride complex $(PCy_3)_2Ru(H)_2Cl_2$ exists in the two distinct diastereomeric forms **18** and **20**.

Comparative investigation of "second-generation" metathesis catalysts: With this panel of NHC-containing ruthenium complexes in hand, we studied their catalytic activity in a representative set of metathesis reactions, focussing our efforts on rather demanding cases.[32]

One of them concerns the formation of the tetrasubstituted cycloalkene **22a,b** which is beyond reach of **1**. As can be seen from Table 2, all NHC-containing complexes effect the cyclization of **21a** (X = NTs) to **22a**, although appreciable differences must be noticed. Thus, the triazol-5-ylidene containing catalyst **11** provides a satisfactory yield of 80% in just 2 h. Prolonged stirring, however, does not lead to further conversion, most likely because of the limited lifetime of complex **11** in solution. In contrast, the *N*-mesityl substituted complex **2** is active over much longer periods, thereby leading to an almost quantitative formation (95%) of the desired product **22a**. Substitution of the backbone of its NHC ligand with two chlorine atoms has surprisingly little effect on the reactivity of the resulting complex **9**, whereas the increased steric bulk of the N-substitutents as in **10** turned out to be disadvantageous. All unsymmetrically substituted NHC complexes **12**, **15**, and **16** are able to effect the cyclization of **21a** to **22a**. However, the catalytic activity of the homologous series **12a–c** shows a significant dependence of the reactivity on the tether length between the alkene entity and the metal core. This effect is likely related to their different capacity to form chelate complexes such as **13** and **14** in situ and is subject to further investigation in this laboratory.

Table 2. Comparison of the reactivity of different NHC complexes in the cyclization of diene **21** to cycloalkene **22**. All reactions have been performed with 5 mol% of the catalyst in toluene at 80°C unless stated otherwise.

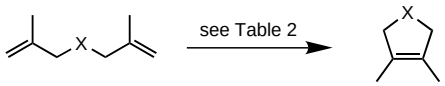

21a: X = NTs
21b: X = $C(COOEt)_2$

22a,b

	Substrate	Catalyst	*t* [h]	Yield [%][a]
1	**21a**	**2**	24	95
2	**21a**	**9**	3	85[c]
3	**21a**	**10**	24	69[b]
4	**21a**	**11**	2	80
5	**21a**	**12a**	24	22
6	**21a**	**12b**	24	48
7	**21a**	**12c**	24	78
8	**21a**	**15**	24	75[c]
9	**21a**	**16**	24	54[c]
10	**21b**	**2**	24	47[c]
11	**21b**	**10**	24	37[c]
12	**21b**	**3**	24	31[d,e]

[a] Isolated Yield unless stated otherwise. [b] In refluxing CH_2Cl_2. [c] GC Yield. [d] Ref. [8b]. [e] Determined by NMR.

The analogous malonate derivative **21b** (X = $C(COOEt)_2$) is more reluctant toward cyclization. Entries 10–12 show that the corresponding cycloalkene **22b** is formed in moderate yields only; in this particular case complex **3**[8b, 27] bearing the saturated NHC is by no means superior to the other catalysts tested.

Care, however, must be taken in generalizing reactivity trends. This becomes clear by comparing the results discussed above with those obtained in the macrocyclization of diene **23** to the musk-odored lactone **24**[33] (Table 3). Whereas complex **10** with the most crowded NHC was clearly inferior to **2** in the formation of the five-membered product **22** (Table 2, entries 1 and 3), it performs better than **2** in this particular macrocyclization (Table 3, entries 1 and 3). The *E*/*Z*-ratio of the resulting product **24**, however, is largely unaffected by the choice of the catalyst.

Table 3. Comparison of the reactivity of different NHC complexes in the cyclization of diene **23** to cycloalkene **24**. All reactions have been performed with 2.5 mol% of the catalyst in refluxing CH_2Cl_2.

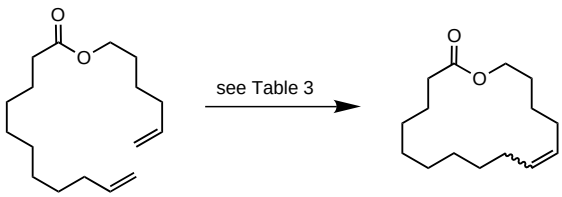

23 **24**

	Catalyst	*t* [h]	GC Yield [%]	*E*/*Z*
1	**2**	3	83	3.4
2	**9**	5	71	3.4
3	**10**	1	84	3.4
4	**11**	5	78	3.3

Another stringent test is the formation of the 14-membered ring lactone **27** containing a trisubstituted double bond. This product is far beyond reach of the parent Grubbs catalyst **1**, which effects only a homo-dimerization of **25** at the least substituted site with formation of an acyclic dimer **26** (Table 4, entry 1). All NHC-containing catalysts, in contrast, furnish the desired macrocycle **27** in good yields (entries 2–5).[34] Entry 5 reveals that complex **3**[8b, 27] containing the "saturated" NHC ligand gives similar results as its "unsaturated" congeners.

Table 4. Comparison of the reactivity of different NHC complexes in the conversion of diene **25** to dimer **26** or the cyclic monomer **27**. All reactions have been performed in refluxing CH_2Cl_2.

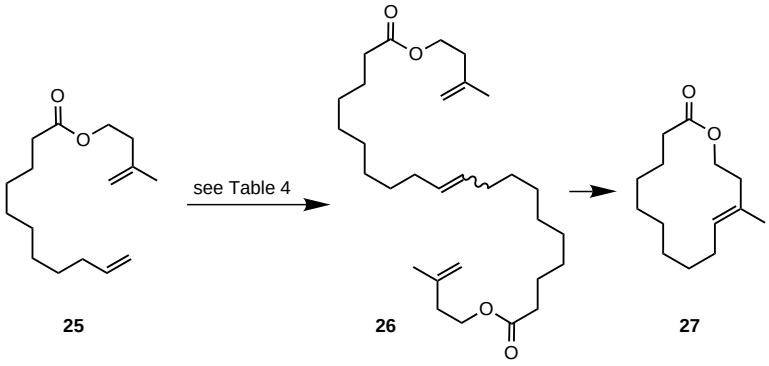

25 **26** **27**

	Catalyst [mol %]	*t* [h]	Product [% Yield]
1	**1** (10%)	17	**26** (79)[a]
2	**2** (10%)	38	**27** (65)[b]
3	**9** (6%)	80	**27** (60)[b]
4	**10** (6%)	40	**27** (57)[b]
5	**3** (6%)	40	**27** (57)[b]

[a] Isolated Yield. [b] GC Yield.

Enyne cycloisomerization reactions provide another excellent forum for evaluating differential reactivity. As in the formation of the tetrasubstituted dihydropyrrole **22a**, complex **2** and its chloro-substituted analogue **9** are almost indistinguishable in their activity toward enyne **28a** (Table 5, entries 1 and 2). It is remarkable, however, that the triazolyl-substituted complex **11** is unable to effect the cycloisomerization of this rather congested substrate (Table 5, entry 4), although it is presently not clear to which extent this failure is due to the limited stability of the complex in solution and/or to an inherent lack of reactivity toward this particular substrate. The less congested enyne **28b** reacts with exceptional ease particularly if complex **10** is used as the catalyst. Note that this preparative result matches the conclusions reached by the IR-thermographic assay method outlined below.

Table 5. Comparison of the reactivity of different NHC complexes in the cycloisomerization of enyne **28** to diene **29**. All reactions have been performed with 5 mol% of the catalyst in toluene at 80 °C unless stated otherwise.

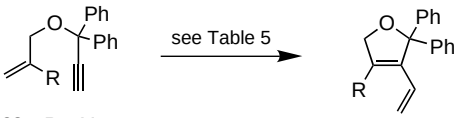

28a: R = Me
28b: R = H

29a,b

	Substrate	Catalyst	*t*	GC Yield [%]
1	**28a**	**2**	18 h	75
2	**28a**	**9**	18 h	74
3	**28a**	**10**	17 h	58
4	**28a**	**11**	24 h	< 5
5	**28b**	**2**	60 min	85[a]
6	**28b**	**10**	5 min	88[a]

[a] Isolated yield.

Taken together, the examples described above unambiguously demonstrate that generalizations concerning the catalytic potency have to be met with caution. More subtle effects including the influence of the solvent on the reactivity of differently substituted ruthenium complexes are operative that cannot be fully rationalized based on our still limited understanding of the mode of action of such "second-generation" catalysts.

Enyne metathesis of sterically demanding substrates: Having identified complexes **2** and **9** as excellent tools for enyne metathesis, we extended this investigation to a diverse set of sterically demanding substrates since previous studies on inter- as well as intramolecular enyne metathesis reactions deal mainly with unhindered cases.[35, 36]

The results compiled in Table 6 illustrate the remarkably wide scope of this type of reaction. Thus, substitutents at the propargylic site are nicely accommodated and do not lower the yields (entries 1–8). Terminal as well as internal alkynes can be employed. Various degrees of substitution of the alkene entities are tolerated and even trisubstituted olefins are found to undergo efficient cycloisomerization in the presence of complex **2**, thereby transferring a dimethylmethylidene unit (cf. **32** → **33**, **44** → **45**). Note that the reactions depicted in entries 2 and 4 lead to the formation of tetrasubstituted alkenes. Catalyst **2** also allows six-membered rings to be formed (entries 9 and 15) and even the seven-membered heterocycle **49** is obtained in excellent yield.[37] The formation of the related product **55**, despite in somewhat lower yield, is particularly noteworthy as the required substrate **54** is an electron deficient and highly conjugated alkyne derivative. To the best of our knowledge, compounds of this type have not yet been used in enyne metathesis reactions mediated by metal carbene complexes.[38]

Catalyst screening by IR thermography—The enyne metathesis case: Recent investigations have demonstrated that high precision IR thermography is a useful tool for the rapid screening of homogeneous and heterogeneous catalysts in parallel.[39, 40] When applied to RCM, this method allowed the catalytic activity to be correlated with the heat uptake from the medium as monitored by the appearance of "cold spots" which are caused, at least in part, by the vaporization of ethylene formed during the reaction.[41] In contrast to RCM, enyne metathesis does not produce any gaseous by-product; therefore it was of interest to study whether this analytical technique can be used to monitor this type of transformation or not.

0947-6539/01/0715-3244 $ 17.50+.50/0 *Chem. Eur. J.* **2001**, *7*, No. 15

Table 6. Cycloisomerization reactions of variously substituted enynes. All reactions were catalyzed by complex **2** (1 mol%) in toluene at 80 °C unless stated otherwise.

	Substrate	Product	*t* [h]	Yield [%]
1	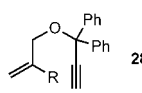 **28**	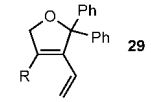 **29**	1	85 (R = H)
2			18	75 (R = Me)[a]
3	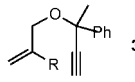 **30**	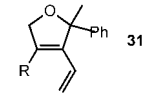 **31**	0.3	80 (R = H)
4			1.5	67 (R = Me)
5	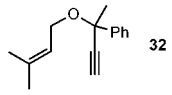 **32**	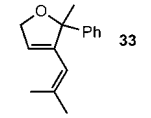 **33**	2.5	77
6	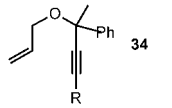 **34**	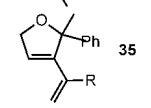 **35**	0.3	93 (R = Me)
7			20	87 (R = Ph)[a]
8	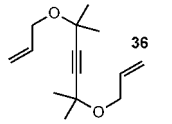 **36**	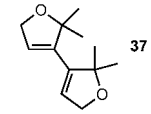 **37**	1	75[a]
9	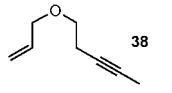 **38**	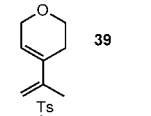 **39**	1	81[b]
10	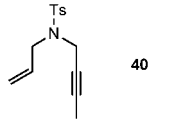 **40**	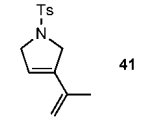 **41**	0.5	97[a]
11	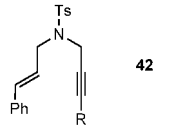 **42**	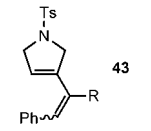 **43**	0.5	81 (R = H)[a]
12			12	67 (R = Me)[a]
13	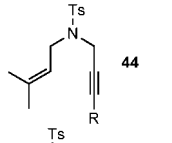 **44**	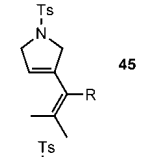 **45**	0.5	89 (R = H)[a]
14			16	20 (R = COOMe)
15	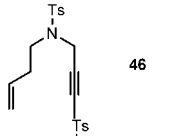 **46**	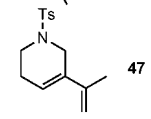 **47**	14	66[a]
16	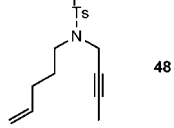 **48**	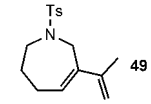 **49**	1.5	81[a]
17	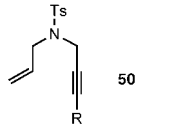 **50**	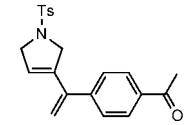 **51**	1	89[a]
	R = C_6H_4COMe			
18	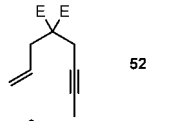 **52**	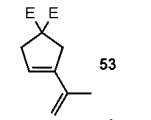 **53**	1.5	89
19	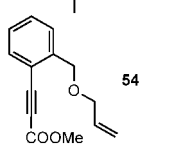 **54**	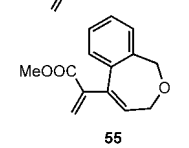 **55**	4	42[a]

[a] Using 5 mol% of the catalyst. [b] Under reflux in CH_2Cl_2; the product was also characterized in form of the cycloadduct prepared by Diels–Alder reaction of diene **39** with dimethyl acetylenedicarboxylate under reflux in toluene (4 h), cf. Experimental Section.

In order to do so, seven wells of a microtiter plate were charged with 40 μL of 0.05 M solutions of catalysts **1**, **2**, **3**, **9**, **10**, **11**, and **56**[5i, 42] in toluene (this corresponds to ≈ 0.6 mol% of catalyst per substrate). Once they are thermostatically set to 30 °C, enyne **28b** (80 μL, thermostatted to 30 °C) was added and the course of the reaction was monitored by the IR camera mounted above the well plate by taking pictures every three seconds. Figure 12 shows the pictures after 9, 51, and 60 s which can be analyzed using the inserted temperature/color code.

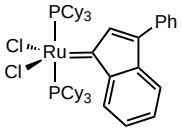

56

Several remarkable features immediately become apparent. Most notable is the *tremendous* exothermicity of this reaction (Scheme 5) when catalyzed by complexes **3** or **10**, causing an increase in temperature (ΔT_{max}) of almost +35 °C. This outcome is in *striking* contrast to the slight endothermicity of $\Delta T_{max} \approx -1$ °C previously observed during RCM.[41] As is clearly visible, this strong evolution of heat even affects the temperature profile of the adjacent wells. Moreover, as the temperature quickly falls off in the thermographs recorded after this very short reaction time, it can be concluded that the transformation of enyne **28b** to diene **29b** is almost finished after only 1 min. This interpretation was confirmed by TLC control, showing no residual starting material but only the essentially quantitative formation of product **29b** after 1 min. Finally, Figure 12 shows that complexes **3** and **10** are roughly equipotent in terms of TOF and are superior to all other catalysts screened in this assay.

A ranking among the remaining catalysts was achieved in a second experiment choosing a narrower temperature window that makes more subtle effects visible. Five vials located sufficiently far apart to minimize mutual heat transfer through the microtiter plate (see above) were charged with the respective catalyst solutions and enyne **28b** as described above and the course of the reaction was followed by IR thermography using a higher precision mode. A prototype picture taken after 210 s (Figure 13) shows that the reaction is well underway if catalysts **9** or **2** are used, while the others clearly stay behind.

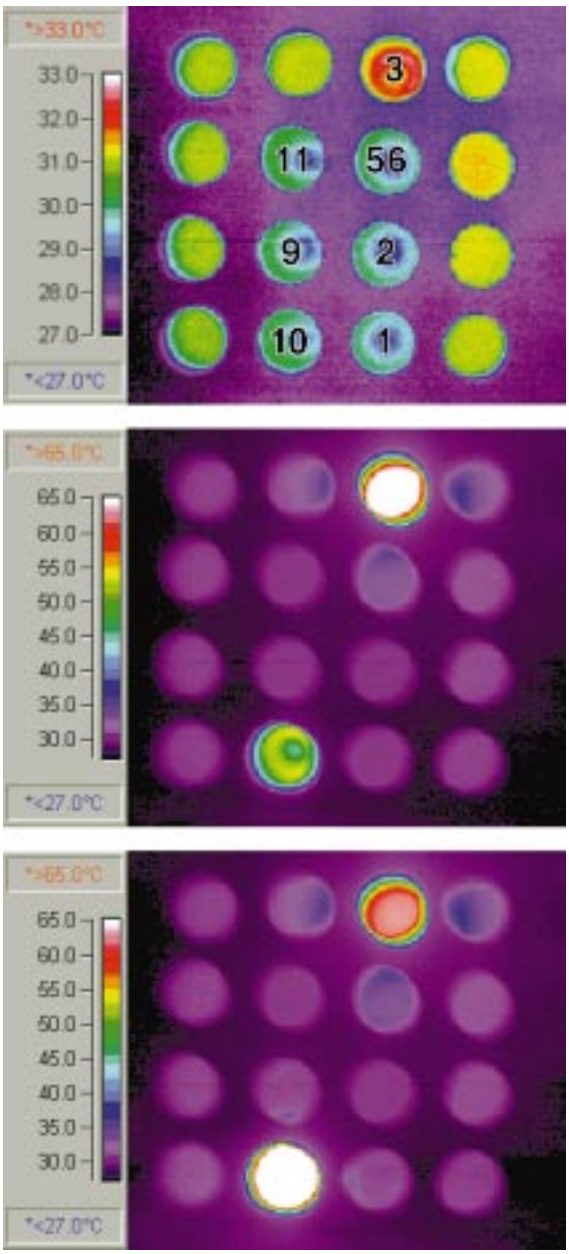

Figure 12. IR-thermographic screening of the enyne metathesis depicted in Scheme 5 catalyzed by complexes **1**, **2**, **3**, **9**, **10**, **11** and **56**. Top: after 9 s; middle: after 51 s; bottom: after 60 s.

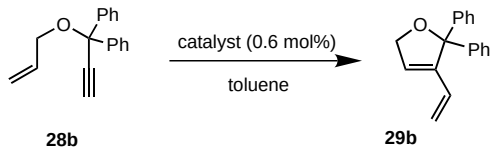

28b **29b**

Scheme 5.

These experiments demonstrate that IR thermography is a convenient and reliable analytical technique for estimating the potency of metathesis catalysts semi-quantitatively. It should be stressed, however, that this assay only screens for *reactivity*; the fastest catalyst, though, does not necessarily provide the highest chemical yield (cf. Table 5). Among other things, the lifetime of the propagating species in solution, that can vary significantly among the series of catalysts screened, also affects the yield obtained. This illustrates that several complementary methods for high throughput screening which allow different preparatively relevant parameters to be assessed are necessary before "combinatorial" catalysis will become a mature field.[40]

Conclusion

The data reported in this paper witness the superiority of NHC containing "second-generation" metathesis catalysts as compared to parent-complex **1**. Equally noteworthy is the fact that different NHC ligands turned out to be optimal for different applications; this shows that no single catalyst outperforms all others in all possible applications. This reinforces the notion that our present understanding of the subtle influences of the substrate on the outcome of a metathesis event is immature and that great care must be taken when generalizing the results obtained from single experiments or a narrow set of test reactions.[32]

Experimental Section

General: All reactions were carried out under Ar in pre-dried glassware using Schlenk techniques. The solvents were dried by distillation over the following drying agents and were transferred under Ar: toluene (Na/K alloy), CH_2Cl_2 (P_4O_{10}), Et_2O (Mg/anthracene), MeOH (Mg), *n*-pentane,

Taken together, these two simple IR-thermographic experiments allow the set of ruthenium-based metathesis catalysts to be ranked according to their individual initiation rates of enyne metathesis ($\mathbf{3} \approx \mathbf{10} \gg \mathbf{9} \approx \mathbf{2} > \mathbf{1} \approx \mathbf{11} \approx \mathbf{56}$). Note that

i) this order is in good qualitative agreement with the results compiled in Table 5 (cf. entries 5 and 6) and
ii) even the seemingly "less" reactive complexes such as **9** or **2** still effect the transformation within just a few minutes.

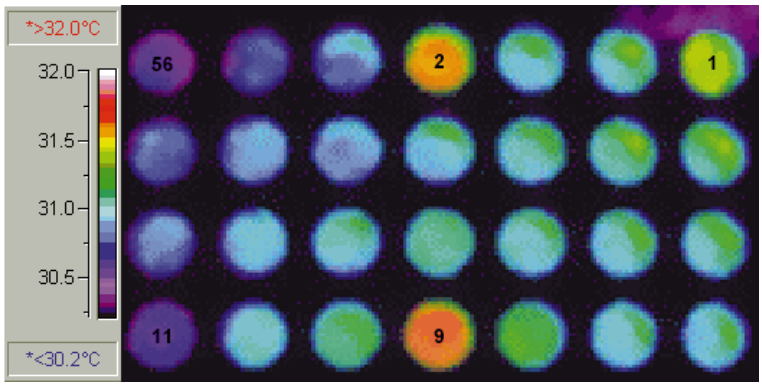

Figure 13. IR-thermographic image recorded over a narrower temperature range (cf. color code) of the enyne metathesis depicted in Scheme 5 catalyzed by complexes **1**, **2**, **9**, and **11** and **56** after 210 s. The wells containing the catalyst solutions are sufficiently far apart to minimize mutual heat transfer, compare text.

0947-6539/01/0715-3246 $ 17.50+.50/0 *Chem. Eur. J.* **2001**, *7*, No. 15

n-hexane (Na/K). Flash chromatography: Merck silica gel 60 (230–400 mesh). NMR: Spectra were recorded on Bruker AC200, AMX300, DPX300 or DMX600 spectrometers in the solvents indicated; chemical shifts (δ) are given in ppm relative to TMS, coupling constants (J) in Hz. IR: Nicolet Magna 750 FT-IR, wavenumbers in cm^{-1}. MS (EI): Finnigan MAT 8200 (70 eV), HR-MS: Finnigan MAT 95. Elemental analyses: Dornis & Kolbe, Mülheim. Equipment for high precision IR thermography: Inframetrics Thermacam (Inframetrics Inc., North Billerica, MA, USA) using the Therma GRAM95 (Inframetrics Inc.) and Dynamite software (Thermoteknix Systems Ltd., Mount Pleasant, Cambridge, UK) for data processing and management. All commercially available substrates were used as received.

Novel imidazolium salts

Compound 7a (X = Br): *N*-Mesitylimidazole (**6**; 1.03 g, 5.56 mmol) and 5-bromo-pent-1-ene (0.83 g, 5.57 mmol) were heated under reflux in toluene (15 mL) for 16 h. Et_2O (30 mL) was added and the suspension filtered. Washing of the precipitate with Et_2O and drying afforded compound **7a** (1.53 g, 82%) as a colorless solid. ^1H NMR (CD_2Cl_2, 300 MHz): $\delta = 10.54$ (s, 1H), 7.89 (s, 1H), 7.28 (s, 1H), 7.04 (s, 2H), 5.84 (m, 1H), 5.07 (d, $J = 19.0$ Hz, 1H), 5.02 (d, $J = 11.1$ Hz, 1H), 4.63 (t, $J = 6.6$ Hz, 2H), 2.34 (s, 3H), 2.30–2.00 (m, 4H), 2.08 (s, 6H); ^{13}C NMR (CD_2Cl_2, 75 MHz): $\delta = 141.3$, 138.3, 136.5, 134.3, 130.8, 129.7, 123.3, 115.9, 49.6, 30.1, 29.5, 20.8, 17.4; IR: $\tilde{\nu} = 3087$, 3065, 2972, 1641, 1605, 1564, 1548, 1450, 1371, 1205, 1159, 1074, 1039, 991, 919, 892, 866, 780, 673 cm^{-1}; MS (ESI): m/z: 255.2 $[M - Br]^+$; elemental analysis calcd for $C_{17}H_{23}BrN_2$ (335.29): C 60.90, H 6.91, N 8.36; found C 61.05, H 7.06, N 8.22.

Compound 7b (X = Br): *N*-Mesitylimidazole (**6**; 1.10 g, 5.89 mmol) and 6-bromo-hex-1-ene (95% pure, 1.12 g, 6.51 mmol) were heated under reflux in toluene (20 mL) for 21 h. Et_2O (50 mL) was added and the suspension was extracted with H_2O (3×50 mL). The aqueous phase was washed with Et_2O (3×50 mL), the solvent was evaporated and the residue dissolved in CH_2Cl_2 (150 mL). Drying over Na_2SO_4 and evaporating of the solvent afforded compound **7b** (1.42 g, 69%) as a colorless solid. ^1H NMR (CD_2Cl_2, 300 MHz): $\delta = 10.48$ (s, 1H), 7.87 (s, 1H), 7.28 (s, 1H), 7.04 (s, 2H), 5.78 (ddt, $J = 17.0$, 10.3, 6.7 Hz, 1H), 5.03 (dq, $J = 17.0$, 1.8 Hz, 1H), 4.96 (dm, $J = 10.3$ Hz, 1H), 4.63 (t, $J = 7.2$ Hz, 2H), 2.34 (s, 3H), 2.20–2.05 (m, 2H), 2.07 (s, 6H), 2.05–1.90 (m, 2H), 1.55–1.40 (m, 2H); ^{13}C NMR (CD_2Cl_2, 75 MHz): $\delta = 141.2$, 138.1, 137.9, 134.3, 130.8, 129.7, 123.3, 122.9, 115.0, 49.9, 32.8, 29.7, 25.2, 20.8, 17.4; IR: $\tilde{\nu} = 3031$, 2973, 2930, 2858, 1639, 1608, 1563, 1544, 1486, 1457, 1379, 1204, 1161, 1068, 1036, 995, 907, 855, 758, 671, 638 cm^{-1}; MS (ESI): m/z: 269.3 $[M - Br]^+$; elemental analysis calcd (%) for $C_{18}H_{25}BrN_2$ (349.31): C 61.89, H 7.21, N 8.02; found C 61.76, H 7.28, N 7.94.

Compound 7c (X = Br): *N*-Mesitylimidazole (**6**; 1.13 g, 6.06 mmol) and 8-bromo-oct-1-ene (1.16 g, 6.06 mmol) were heated under reflux in toluene (15 mL) for 16 h. Et_2O (30 mL) was added and the suspension filtered. Washing with Et_2O and drying of the residue in vacuo afforded compound **7c** (1.40 g, 61%) as a colorless solid. ^1H NMR (CD_2Cl_2, 300 MHz): $\delta =$ 10.54 (t, $J = 1.5$ Hz, 1H), 7.84 (t, $J = 1.9$ Hz, 1H), 7.28 (t, $J = 1.9$ Hz, 1H), 7.04 (s, 2H), 5.79 (ddt, $J = 17.2$, 10.2, 6.7 Hz, 1H), 4.98 (dm, $J = 17.2$ Hz, 1H), 4.91 (dm, $J = 10.2$ Hz, 1H), 4.61 (t, $J = 7.2$ Hz, 2H), 2.34 (s, 3H), 2.08 (s, 6H), 2.05–1.95 (m, 4H), 1.45–1.30 (m, 6H); ^{13}C NMR (CD_2Cl_2, 75 MHz): $\delta = 141.2$, 138.9, 138.2, 134.3, 130.8, 129.7, 123.3, 122.8, 114.1, 50.1, 33.5, 30.3, 28.6, 28.4, 25.9, 20.8, 17.4; IR: $\tilde{\nu} = 3058$, 2974, 2929, 2850, 1639, 1608, 1564, 1543, 1486, 1460, 1379, 1203, 1157, 1065, 905, 854, 822, 662, 634 cm^{-1}; MS (ESI): m/z: 297.2 $[M - Br]^+$; elemental analysis calcd for $C_{20}H_{29}BrN_2$ (377.37): C 63.66, H 7.75, N 7.42; found C 63.48, H 7.82, N 7.35.

Compound 7d (X = Br): *N*-Mesitylimidazole (**6**; 0.78 g, 4.17 mmol) and (2-bromo-ethoxy)-*tert*-butyl-dimethyl-silane (1.00 g, 4.17 mmol) were heated under reflux in toluene (15 mL) for 16 h. Et_2O (30 mL) was added and the suspension was extracted with H_2O (3×50 mL). The aqueous phase was washed with Et_2O (3×50 mL). The solvent was evaporated and the residue dissolved in CH_2Cl_2 (20 mL). Drying over Na_2SO_4 and evaporating of the solvent afforded compound **7d** (0.50 g, 28%) as a colorless solid. ^1H NMR (CD_2Cl_2, 300 MHz): $\delta = 10.31$ (s, 1H), 7.86 (s, 1H), 7.22 (s, 1H), 7.05 (s, 2H), 4.82 (t, $J = 4.7$ Hz, 2H), 4.09 (t, $J = 4.7$ Hz, 2H), 2.35 (s, 3H), 2.08 (s, 6H), 0.87 (s, 9H), 0.06 (s, 6H); ^{13}C NMR (CD_2Cl_2, 75 MHz): $\delta = 141.3$, 138.1, 134.4, 130.8, 129.7, 124.0, 122.4, 62.1, 52.5, 25.6, 20.8, 18.0, 17.4, −5.8; IR: $\tilde{\nu} = 3034$, 2955, 2927, 2855, 1609, 1566, 1547, 1487, 1471, 1447, 1385, 1362, 1259, 1203, 1164, 1110, 1067, 1036, 1007, 937, 829, 812, 780, 731, 668, 640 cm^{-1}; MS (ESI): m/z: 345.2 $[M - Br]^+$; elemental analysis calcd for $C_{20}H_{33}BrN_2OSi$ (425.48): C 56.46, H 7.82, N 6.58; found: C 56.23, H 8.06, N 6.98.

Compound 7e (X = I): *N*-Mesitylimidazole (**6**; 1.29 g, 6.90 mmol) and 1,1,1,2,2,3,3,4,4,5,5,6,6-tridecafluoro-8-iodo-octane (3.31 g, 6.98 mmol) were heated under reflux in toluene (20 mL) for 4 d. Evaporation of the solvent and crystallization (THF/methyl *tert*-butylether) of the residue afforded compound **7e** (3.50 g, 77%) as a pale yellow solid. ^1H NMR (CD_2Cl_2, 300 MHz): $\delta = 10.12$ (s, 1H), 8.07 (s, 1H), 7.28 (s, 1H), 7.06 (s, 2H), 5.13 (t, $J = 6.3$ Hz, 2H), 3.07 (tt, $J = 18.6$, 6.2 Hz, 2H), 2.36 (s, 3H), 2.08 (s, 6H); ^{13}C NMR (CD_2Cl_2, 75 MHz): $\delta = 141.7$, 137.9, 134.3, 130.5, 129.8, 123.7, 123.4, 122.0–105.0 (m, CF_x), 43.1 (t, $J = 21.3$ Hz), 20.9, 17.5; IR: $\tilde{\nu} = 3120$, 3008, 1610, 1566, 1551, 1319, 1236, 1206, 1144, 1121, 1079, 853, 747, 708 cm^{-1}; MS (ESI): m/z: 1193 $[2M - I]^+$, 533 $[M - I]^+$; elemental analysis calcd for $C_{20}H_{18}F_{13}IN_2$ (660.25): C 36.38, H 2.75, N 4.24; found: C 36.32, H 2.81, N 4.21.

Metathesis pre-catalysts: Where assignments of the signals [based on COSY, DEPT and 2D ^1H,^{13}C-chemical shift correlated spectra (HSQC and HMBC)] are given, they are unambiguous and refer to the arbitrary numbering schemes shown in the inset.

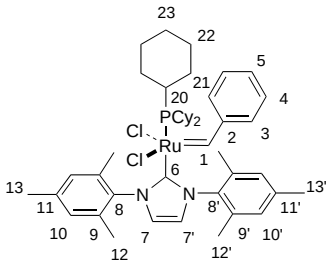

Complex 2: Complex **1** (4.60 g, 5.59 mmol) and carbene **5a** (2.43 g, 7.98 mmol) were stirred in toluene (100 mL) under Ar at room temperature for 1 h. The solvent was evaporated and *n*-pentane (100 mL) was added. The precipitate was filtered off, washed with *n*-pentane and dried in vacuo to afford complex **2** (3.58 g, 76%) as a violet solid. ^1H NMR (CD_2Cl_2, 600 MHz): $\delta = 19.40$ (s, 1H, 1-H), 8.90 (br, 1H, 3a-H), 7.40 (t, $J = 7.3$ Hz, 1H, 5-H), 7.15 (br, 1H, 3b-H), 7.13 (t, 2H, 4-H), 7.05 (s, 2H, 10-H), 6.99 (s, 2H, 7-H, 7′-H′), 6.75 (br, 1H, 10′-H), 5.95 (br, 1H, 10′-H), 2.43 (br, 6H, 12-H), 2.35 (s, 3H, 13-H), 2.21 (m, 3H, 20-H), 2.20 (br, 3H, 12′-H), 1.96 (s, 3H, 13′-H), 1.90 (m, 3H, 12′-H), 1.53 (m, 3H, 23eq-H), 1.51 (m, 6H, 22eq-H), 1.39 (m, 6H, 21eq-H), 1.03 (m, 9H, 22ax-H, 23ax-H), 0.93 (m, 6H, 21ax-H); ^{13}C NMR (CD_2Cl_2, 151 MHz): $\delta = 295.3$ (d, $J_{CH} = 147$ Hz, C-1), 189.7 (s, $J_{CP} = 83.0$ Hz, C-6), 152.1 (s, C-2), 139.5 (s, C-11), 138.8 (s, C-11′), 138.3 (s, C-9), 137.1 (s, C-8′), 136.4 (s, C-9′), 135.9 (s, C-8), 129.7 (d, $J_{CH} = 157$ Hz, C-10), 129.0 (d, C-10′), 128.2 (d, $J_{CH} = 158$ Hz, C-5), 128.1 (d, C-4), 125.2 (d, $^1J_{CH} = 196$ Hz, $^2J_{CH} = 12$ Hz, $J_{CP} = 2.8$ Hz, C-7), 124.7 (d, $^1J_{CH} = 196$ Hz, $^2J_{CH} = 12$ Hz, $J_{CP} = 1.6$ Hz), 31.9 (d, $^1J_{CH} = 127$ Hz, $J_{CP} = 17$ Hz, C-7′, C-20), 29.5 (t, $^1J_{CH} = 129$ Hz, C-21), 28.2 (t, $^1J_{CH} = 128$ Hz, $J_{CP} = 10$ Hz, C-22), 26.7 (t, $^1J_{CH} = 127$ Hz, C-23), 21.3 (q, $^1J_{CH} = 127$ Hz, C-13), 21.1 (q, $^1J_{CH} =$ 126 Hz, C-13′), 19.7 (q, $^1J_{CH} = 128$ Hz, C-12), 18.4 (q, $^1J_{CH} = 127$ Hz, C-12′); ^{31}P NMR (CD_2Cl_2, 243 MHz): $\delta = 31.9$.

^1H NMR (C_6D_6, 600 MHz): $\delta = 19.92$ (s, 1H, 1-H), 9.30 (br, 1H, H-3), 7.40 (br, 1H, H-3), 7.16 (t, 1H, $J = 7.3$ Hz, 5-H), 6.99 (m, 2H, 4-H), 6.91 (s, 2H, 10-H), 6.23 (d, $J = 1.8$ Hz, 1H, 7′-H), 6.20 (dd, 1H, $J_{7,7'} = 1.8$ Hz, $J_{7,P} =$ 0.8 Hz, 7-H), 6.20 (br, 2H, H-10′), 2.65 (br, 6H, 12-H), 2.51 (dt, 3H, $J_{20,P} = 11.2$, $J_{20,21ax} = 9.6$ Hz, 20-H), 2.22 (br, 6H, 12′-H), 2.20 (s, 3H, 13-H), 1.85 (s, 3H, 13′-H), 1.66 (br, 6H, H-21_{eq}), 1.57 (m, 6H, H-22_{eq}), 1.54 (d, $J =$ 12.6 Hz, 3H, H-23_{eq}), 1.14 (m, 12H, H-21_{ax}, H-22_{ax}), 1.06 (m, 3H, H-23_{ax}); ^{13}C NMR (C_6D_6, 151 MHz): $\delta = 295.4$ (d, $J_{CH} = 148$ Hz, C-1), 190.7 (s, $J_{CP} =$ 83.6 Hz, C-6), 152.4 (s, C-2), 139.0 (s, C-11), 138.5 (s, C-9), 138.3 (s, C-11′), 137.3 (s, C-8′), 136.5 (s, C-9′), 136.1 (s, C-8), 129.7 (d, $J_{CH} = 157$ Hz, C-10), 128.9 (d, C-10′), 128.0 (m, C-4), 127.8 (d, C-5), 124.6 (d, $^1J_{CH} = 196$ Hz, $^2J_{CH} = 12$ Hz, $J_{CP} = 2.8$ Hz, C-7), 124.1 (d, $^1J_{CH} = 196$ Hz, $^2J_{CH} = 12$ Hz, $J_{CP} =$ 1.5 Hz, C-7′), 32.1 (d, $^1J_{CH} = 126$ Hz, $J_{CP} = 17$ Hz, C-20), 29.7 (t, $^1J_{CH} =$ 128 Hz, C-21), 28.2 (t, $^1J_{CH} = 124$ Hz, $J_{CP} = 10$ Hz, C-22), 26.6 (t, $^1J_{CH} =$ 128 Hz, C-23), 21.2 (q, $^1J_{CH} = 126$ Hz, C-13), 21.0 (q, $^1J_{CH} = 126$ Hz, C-13′), 20.1 (q, $^1J_{CH} = 128$ Hz, C-12), 18.7 (q, $^1J_{CH} = 129$ Hz, C-12′); ^{31}P NMR (C_6D_6, 243 MHz): $\delta = 31.8$; IR: $\tilde{\nu} =$ 3165, 3131, 2921, 2849, 1608, 1570, 1485, 1445, 1314, 1264, 1242, 1174, 1037, 1005, 898, 848, 740, 701, 686 cm^{-1}.

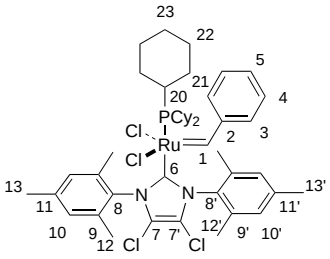

Complex 9: Complex **1** (402 mg, 0.49 mmol) and carbene **5c** (241 mg, 0.65 mmol) were stirred in toluene (25 mL) under Ar at room temperature for 1 h. The solvent was evaporated and *n*-pentane (10 mL) was added. The precipitate formed was filtered off, washed with *n*-pentane and dried in vacuo affording complex **9** (387 mg, 87%) as a violet-brownish solid. Alternatively the purification can be performed by flash chromatography (*n*-pentane/Et_2O 4:1 → 2:1) affording **9** in 79% yield. ^1H NMR (CD_2Cl_2, 600 MHz): $\delta = 19.39$ (s, 1H, 1-H), 8.90 (br, 1H, 3a-H), 7.43 (t, 1H, $J =$ 7.3 Hz, 5-H), 7.15 (t, 2H, $J = 7.6$ Hz, 4-H), 7.10 (br, 1H, 3b-H), 7.09 (s, 1H, 10-H), 6.80 (br, 1H, 10′-H), 5.95 (br, 1H, 10′-H), 2.41 (br, 6H, 12-H), 2.38 (s, 3H, 13-H), 2.19 (m, 3H, 20-H), 2.18 (br, 3H, 12′-H), 1.97 (s, 3H, 13′-H), 1.87 (br, 3H, 12′-H), 1.53 (m, 3H, 23eq-H), 1.51 (m, 6H, 22eq-H), 1.37 (m, 6H, 21eq-H), 1.03 (m, 9H, 22ax-H, 23ax-H), 0.91 (m, 6H, 21ax-H); ^{13}C NMR (CD_2Cl_2, 151 MHz): $\delta = 298.0$ (d, $^1J_{CH} = 148$ Hz, $J_{CP} = 9$ Hz, C-1), 192.7 (s, $^1J_{CP} = 85.2$ Hz, C-6), 152.1 (s, C-2), 140.8 (s, C-11), 140.0 (s, C-11′), 139.2 (s, C-9′), 137.1 (s, C-9), 134.1 (s, C-8′), 132.4 (s, C-8), 130.0 (d, $^1J_{CH} =$ 158 Hz, C-10), 129.2 (d, $^1J_{CH} = 156$ Hz, C-10′), 128.7 (d, $^1J_{CH} = 129$ Hz, C-5), 128.2 (d, C-4), 119.3 (s, $J_{CP} = 2.3$ Hz, C-7′), 119.1 (s, $J_{CP} = 4.1$ Hz, C-7), 31.9 (d, $^1J_{CH} = 129$ Hz, $J_{CP} = 17.5$ Hz, C-20), 29.5 (t, $^1J_{CH} = 128$ Hz, C-21), 28.1 (t, $^1J_{CH} = 128$ Hz, $J_{CP} = 10.0$ Hz, C-22), 26.5 (t, $^1J_{CH} = 126$ Hz, C-23), 21.4 (q, $^1J_{CH} = 127$ Hz, C-13), 21.2 (q, $^1J_{CH} = 127$ Hz, C-13′), 19.8 (q, $^1J_{CH} = 128$ Hz, C-12), 18.5 (q, $^1J_{CH} = 127$ Hz, C-12′); ^{31}P NMR (CD_2Cl_2, 243 MHz): $\delta =$ 31.7; IR: $\tilde{\nu} = 3052$, 2927, 2847, 1608, 1568, 1559, 1523, 1483, 1444, 1357, 1294, 1244, 1174, 1037, 899, 854, 818, 747, 734 cm^{-1}; MS (ESI): m/z: 881.5 $[M - Cl]^+$; elemental analysis calcd for $C_{46}H_{61}Cl_4N_2PRu$ (915.86): C 60.33, H 6.71, N 3.06; found C 60.19, H 6.65, N 3.12.

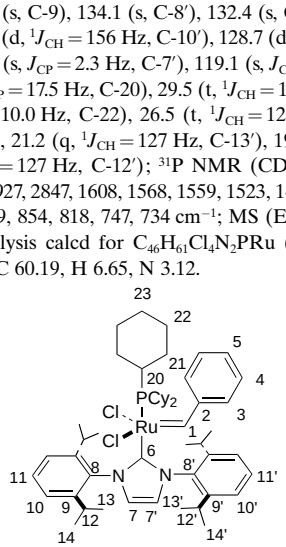

Complex 10: Complex **1** (485 mg, 0.59 mmol) and carbene **5b** (275 mg, 0.71 mmol) were stirred in toluene (30 mL) under Ar at 50 °C for 2 h. The solvent was evaporated and *n*-pentane (10 mL) was added. The precipitate formed was filtered off at −78 °C, washed with *n*-pentane (−78 °C) and dried in vacuo affording product **10** (450 mg, 82%) as a violet solid. Alternatively, the purification of the crude product can be achieved by flash chromatography (*n*-pentane/Et_2O 4:1), affording complex **9** (376 mg, 69%) as a violet solid. ^1H NMR (CD_2Cl_2, 600 MHz): $\delta = 19.62$ (s, 1H, 1-H), 7.98 (br, 2H, 3-H), 7.50 (t, $J = 7.6$ Hz, 1H, 11-H), 7.40 (d, $J = 7.7$ Hz, 2H, 10-H), 7.33 (tt, $J = 7.3$, 1.1 Hz, 1H, 5-H), 7.10 (s, 1H, 7-H), 7.05 (s, 1H, 7′-H), 7.05 (s, 2H, 4-H), 6.84 (t, 1H, $J = 7.5$ Hz, 11′-H), 6.79 (m, 2H, 10′-H), 3.55 (sept, 2H, $J = 6.6$ Hz, 12-H), 3.10 (m, 2H, 12′-H), 2.11 (m, 3H, 20-H), 1.50 – 1.45 (m, 9H, 22eq-H, 23eq-H), 1.40 (d, 6H, $J = 6.6$ Hz, 13-H), 1.37 (m, 6H, 21eq-H), 1.29 (d, 6H, 13′-H), 1.08 (d, 6H, $J = 6.8$ Hz, 14-H), 1.00 – 0.95 (m, 15H, 21ax-H, 22ax-H, 23ax-H), 0.95 (d, 6H, $J = 7.1$ H, 14′-Hz); ^{13}C NMR (CD_2Cl_2, 151 MHz): $\delta = 296.7$ (d, $^1J_{CH} = 148$ Hz, $J_{CP} = 9$ Hz, C-1), 190.3 (s, $J_{CP} = 83.8$ Hz, C-6), 151.6 (s, C-2), 148.7 (s, C-9), 146.2 (s, C-9′), 137.6 (s, C-8′), 136.0 (s, C-8), 131.6 (d, $^1J_{CH} = 132$ Hz, C-3), 131.3 (d, $^1J_{CH} = 160$ Hz, C-11), 130.0 (d, $^1J_{CH} = 159$ Hz, C-11′), 128.2 (d, $^1J_{CH} = 158$ Hz, C-5), 128.0 (d, $^1J_{CH} = 159$ Hz, C-4), 126.3 (d, $^1J_{CH} = 197$ Hz, C-7), 126.1 (d, $^1J_{CH} =$ 196 Hz, C-7′), 124.2 (d, $^1J_{CH} = 160$ Hz, C-10), 123.7 (d, $^1J_{CH} = 158$ Hz, C-10′), 32.2 (d, $^1J_{CH} = 126$ Hz, $J_{CP} = 17$ Hz, C-20), 29.5 (t, $^1J_{CH} = 128$ Hz, C-21), 29.2 (d, C-12), 28.2 (d, C-12′), 28.1 (t, $^1J_{CH} = 127$ Hz, $J_{CP} = 10$ Hz, C-22), 26.9 (q, C-14), 26.6 (t, $^1J_{CH} = 124$ Hz, C-23), 26.3 (q, $^1J_{CH} = 126$ Hz, C-14′), 22.9 (q, $^1J_{CH} = 125$ Hz, C-13), 22.3 (q, $^1J_{CH} = 125$ Hz, C-13′); ^{31}P NMR (CD_2Cl_2, 243 MHz): $\delta = 29.8$; IR: $\tilde{\nu} = 3166$, 3123, 3093, 3060, 2962, 2925, 2962, 2849, 1590, 1569, 1445, 1321, 1305, 1173, 1117, 897, 847, 757, 739, 686 cm^{-1}; MS (ESI): m/z: 895.7 $[M - Cl]^+$; elemental analysis calcd for $C_{52}H_{75}Cl_2N_2PRu$ (931.13): C 67.08, H 8.12, N 3.01; found C 67.05, H 8.20, N 2.96.

Complex 11: Complex **1** (307 mg, 0.37 mmol) and commercially available 1,3,4-triphenyl-4,5-dihydro-1*H*-1,2,4-triazol-5-ylidene (96%, 128 mg, 0.41 mmol)[21] were stirred in toluene (15 mL) under Ar at room temperature for 1 h. The solvent was evaporated and the residue was purified by flash chromatography (*n*-hexane/Et_2O 4:1 → 2:1 → 1:1) affording complex **11** (269 mg, 86%) as a brown solid. ^1H NMR (CD_2Cl_2, 600 MHz): $\delta = 19.57$ (d, 1H, $J_{HP} = 8.2$ Hz, Ru=C*H*), 19.38 (d, 1H, $J_{HP} = 6.3$ Hz, Ru=C*H*), 8.21 (d, 1H, $J = 8.4$ Hz, *o*-Ph), 7.90 – 7.80 (br, 1H), 7.85 (d, $J = 7.0$ Hz, 1H, *o*-Ph), 7.71 (t, 1H, 7.5 Hz, *m*-Ph), 7.59 (t, $J = 6.8$ Hz, 1H, *m*-Ph), 7.57 (m, 1H, *p*-Ph), 7.55 (m, 1H), 7.50 – 7.38 (m, 4H), 7.33 – 7.25 (m, 2H), 7.19 (t, 1H, $J = 8.2$ Hz, *m*-Ph), 7.16 (m, 1H, *o*-Ph), 7.10 (m, 1H), 7.08 – 7.02 (m, 1H), 7.06 (m, 1H), 7.00 (m, 1H), 6.85 (br, 1H), 2.11 (m, 3H, PCy_3), 1.70 – 1.50 (m, 15H, PCy_3-H_{eq}), 1.35 – 1.00 (m, 15H, PCy_3-H_{ax}); ^{13}C NMR (CD_2Cl_2, 150 MHz): $\delta = 291.9$ (Ru=*C*H), 192.6 ($J_{CP} = 88.6$ Hz, Ru=*C*N_2), 191.0 ($J_{CP} = 92.4$ Hz, Ru=*C*N_2), 154.7 ($J_{CP} = 2.8$ Hz), 153.8 ($J_{CP} = 3.4$ Hz), 151.1, 150.9, 142.4, 141.6, 33.0 ($J_{CP} = 16.3$ Hz, P*C*H), 32.9 ($J_{CP} = 16.1$ Hz,P*C*H), 29.3, 29.3, 28.0 ($J_{CP} =$ 9.7 Hz), 28.0 ($J_{CP} = 9.9$ Hz), 26.6, 26.6; ^{31}P NMR (CD_2Cl_2, 243 MHz): $\delta =$ 24.3, 23.5; IR (KBr): $\tilde{\nu} = 3063$, 2923, 2849, 1595, 1554, 1495, 1445, 1370, 1201, 1176, 1128, 916, 885, 846, 817, 760, 694, 687 cm^{-1}; MS (ESI): m/z: 804.2 $[M - Cl]^+$; elemental analysis calcd for $C_{45}H_{54}Cl_2N_3PRu$ (839.89): C 64.35, H 6.48, N 5.00; found: C 64.51, H 6.55, N 4.94.

Complex 12a: The imidazolium salt **7a** (316 mg, 0.94 mmol), KO*t*Bu (94 mg, 0.88 mmol) and complex **1** (646 mg, 0.79 mmol) were stirred in toluene (40 mL) for 3 h under Ar at room temperature. The suspension was filtered and the solvent evaporated in vacuo. Flash chromatography (*n*-pentane/Et_2O 4:1 → CH_2Cl_2/Et_2O 4:1) afforded complex **12a** (263 mg, 42%) as a red solid. ^1H NMR (CD_2Cl_2, 200 MHz): $\delta = 19.22$ (s, 1H), 7.87 (br, 2H), 7.50 – 7.35 (m, 1H), 7.30 – 7.20 (m, 1H), 7.13 (t, 2H, $J = 7.5$ Hz), 6.85 (d, 1H, $J = 1.9$ Hz), 6.40 – 6.20 (br, 2H), 5.97 (m, 1H, $J = 17.1$, 10.4 Hz), 5.15 (m, 1H, $J = 17$ Hz), 5.08 (m, 1H, $J = 10.4$ Hz), 4.72 (t, 2H, $J = 7$ Hz), 2.40 – 2.25 (m, 3H), 2.34 (s, 3H), 2.25 – 2.10 (m, 2H), 1.93 (s, 6H), 1.95 – 1.85 (m, 2H), 1.80 – 1.50 (m, 15H), 1.45 – 1.00 (m, 15H); ^{31}P NMR (CD_2Cl_2, 81 MHz): $\delta = 34.0$; IR: $\tilde{\nu} = 3161$, 3124, 2925, 2849, 1639, 1608, 1589, 1490, 1445, 1408, 1238, 1173, 1005, 895, 737, 687 cm^{-1}; MS (ESI): m/z: 795.5 $[M]^+$, 761.5 $[M - Cl]^+$; elemental analysis calcd for $C_{42}H_{61}Cl_2N_2PRu$ (796.91): C 63.30, H 7.72, N 3.52; found C 63.26, H 7.66, N 3.48.

Complex 12b: Imidazolium salt **7b** (162 mg, 0.42 mmol), KO*t*Bu (53 mg, 0.47 mmol) and complex **1** (328 mg, 0.40 mmol) were stirred in toluene (25 mL) for 3 h at room temperature under Ar. The suspension was filtered and the solvent was evaporated. Flash chromatography (*n*-pentane/Et_2O 4:1 → CH_2Cl_2/Et_2O 4:1) afforded complex **12b** (132 mg, 41%) as a red solid. ^1H NMR (CD_2Cl_2, 200 MHz): $\delta = 19.23$ (s, 1H), 7.86 (br, 2H), 7.42 (t, 1H, $J = 7.1$ Hz), 7.27 (s, 1H), 7.13 (t, 2H, $J = 7.8$ Hz), 6.84 (s, 1H), 6.40 – 6.20 (br, 2H), 5.89 (ddt, 1H, $J = 17.1$, 10.4, 6.7 Hz), 5.08 (dm, 1H, $J = 17.1$ Hz), 5.02 (dm, 1H, $J = 10.3$ Hz), 4.70 (t, 2H, $J = 7.5$ Hz), 2.40 – 2.15 (m, 5H), 2.34 (s, 3H), 2.00 – 1.80 (m, 2H), 1.93 (s, 6H), 1.80 – 1.50 (m, 15H), 1.45 – 1.00 (m, 17H); ^{31}P NMR (CD_2Cl_2, 81 MHz): $\delta = 34.2$; IR: $\tilde{\nu} = 3161$, 3123, 3096, 2925, 2849, 1640, 1490, 1445, 1409, 1240, 1173, 1004, 913, 895, 847, 741, 687 cm^{-1}; MS (ESI): m/z: 775.5 $[M - Cl]^+$; elemental analysis calcd for $C_{43}H_{63}Cl_2N_2PRu$ (810.93): C 63.69, H 7.83, N 3.45; found C 63.78, H 7.89, N 3.42.

Complex 12c: Imidazolium salt **7c** (172 mg, 0.46 mmol), KO*t*Bu (51 mg, 0.46 mmol) and complex **1** (281 mg, 0.34 mmol) were stirred in toluene (20 mL) for 1.5 h at room temperature under Ar. The suspension was filtered and the solvent was evaporated. Flash chromatography (*n*-pentane/Et_2O 4:1) afforded **12c** (115 mg, 40%) as a red solid. ^1H NMR (CD_2Cl_2, 200 MHz): $\delta = 19.24$ (s, 1H), 7.84 (br, 2H), 7.42 (t, 1H, $J = 7.2$ Hz), 7.30 – 7.20 (br, 1H), 7.12 (t, 2H, $J = 7.5$ Hz), 6.84 (s, 1H), 6.40 – 6.20 (br, 2H), 5.85 (ddt, 1H, $J = 17.1$, 10.4, 6.7 Hz), 5.02 (dm, 1H, $J = 17.1$ Hz), 4.90 (dm, 1H, $J = 10.4$ Hz), 4.68 (t, 2H, $J = 7.7$ Hz), 2.40 – 1.00 (m, 43H), 2.34 (s, 3H), 1.93 (s, 6H); ^{31}P NMR (CD_2Cl_2, 81 MHz): $\delta = 34.1$; IR: $\tilde{\nu} = 3160$, 3123, 3092, 3056, 2925, 2850, 1640, 1609, 1589, 569, 1489, 1446, 1173, 1004, 913, 896, 847, 741, 687 cm^{-1}; MS (ESI): m/z: 803.3 $[M - Cl]^+$; elemental analysis calcd for $C_{45}H_{67}Cl_2N_2PRu$ (838.99): C 64.42, H 8.05, N 3.34; found C 64.56, H 8.14, N 3.42.

0947-6539/01/0715-3248 $ 17.50+.50/0 *Chem. Eur. J.* **2001**, *7*, No. 15

Complex 13: Complex **12b** (30 mg, 0.04 mmol) was heated under reflux in *n*-pentane (70 mL) for 1 h. The suspension was filtered and the solvent was slowly evaporated affording complex **13** (20 mg, 77%) as a brown crystalline solid. ^{1}H NMR (CD_2Cl_2, 200 MHz): $\delta = 20.22$ (dt, 1H, $J = 9.8$, 4.9 Hz), 7.08 (dm, 1H, $J = 1.8$ Hz), 6.99 (s, 2H), 6.83 (s, 1H), 3.56 (tm, 2H, $J = 4.9$ Hz), 2.93 (m, 2H), 2.35–2.10 (m, 5H), 2.33 (s, 3H), 2.27 (s, 6H), 1.85–1.60 (m, 17H), 1.55–1.10 (m, 15H); ^{31}P NMR (CD_2Cl_2, 81 MHz): $\delta =$ 29.1; IR: $\tilde{\nu} = 3123$, 2924, 2852, 1609, 1569, 1485, 1462, 1448, 1405, 1387, 1160, 885, 852, 733, 698 cm^{-1}; MS (ESI): *m*/*z*: 706.3 $[M]^+$; elemental analysis calcd for $C_{35}H_{55}Cl_2N_2PRu$ (706.78): C 59.48, H 7.84, N 3.96; found C 59.36, H 7.88, N 4.02.

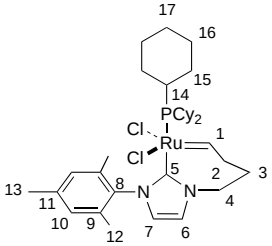

Complex 14: Complex **12a** (25 mg, 0.03 mmol) was heated under reflux in *n*-hexane (50 mL) for 45 min. The suspension was filtered and the filtrate was slowly evaporated affording chelate complex **14** (17 mg, 78%) as a brown crystalline solid. ^{1}H NMR (CD_2Cl_2, 600 MHz): $\delta = 19.55$ (dt, 1H, 1-H, $^3J_{1,P} = 13.6$ Hz, $^3J_{1,2} = 6.3$ Hz), 7.08 (dd, 1H, 6-H, $^3J_{6,7} = 1.8$ Hz, $^3J_{6,P} =$ 0.7 Hz), 7.00 (s, 2H, 10-H), 6.84 (dd, dd, 7-H, 1H, $^3J_{7,6} = 1.8$ Hz, $^3J_{7,P} =$ 0.9 Hz), 3.83 (dd, 2H, 4-H, $^3J > 6.3$ Hz, $^3J < 6.3$ Hz), 3.58 (q, 2H, 2-H, $^3J_{2,1} = 6.6$ Hz (d), $^3J_{2,3} = 6.6$ Hz (t)), 2.32 (s, 3H, 13-H), 2.30 (m, 2H, 3-H), 2.22 (s, 6H, 12-H), 2.18 (m, 3H, 14-H), 1.81 (m, 6H, 15eq-H), 1.72 (m, 6H, 16eq-H), 1.66 (m, 3H, 17eq-H), 1.51 (m, 6H, 15ax-H), 1.19 (m, 3H, 17ax-H), 1.16 (m, 6H, 22ax-H); ^{13}C NMR (CD_2Cl_2, 150 MHz): $\delta = 334.4$ ($J_{CP} =$ 159.3 Hz, C-1), 183.1 ($J_{CP} = 109.4$ Hz, C-5), 138.4 (C-11), 137.0 (C-8), 136.8 (C-9), 129.0 (C-10), 122.5 ($J_{CP} = 3.2$ Hz, C-6*), 122.2 ($J_{CP} = 3.1$ Hz, C-7*), 57.4 (C-2), 47.9 (C-4), 32.7 ($J_{CP} = 15.0$ Hz, C-14), 29.9 (C-15), 28.8 ($J_{CP} =$ 9.8 Hz,C-16), 26.7 (C-17), 24.1 (C-3), 21.0 (C-13), 19.3 (C-12); ^{31}P NMR (CD_2Cl_2, 243 MHz): $\delta = 22.8$; IR: $\tilde{\nu} = 3124$, 2921, 2850, 1609, 1562, 1487, 1446, 1407, 1259, 1172, 1005, 888, 851, 730, 700 cm^{-1}; MS (ESI): *m*/*z*: 657.3 $[M - Cl]^+$; elemental analysis calcd for $C_{34}H_{53}Cl_2N_2PRu$ (692.76): C 58.95, H 7.71, N 4.04; found C 59.11, H 7.65, N 4.01.

Complex 15: Imidazolium salt **7d** (170 mg, 0.40 mmol), KO*t*Bu (45 mg, 0.40 mmol) and complex **1** (270 mg, 0.33 mmol) were stirred in toluene (25 mL) for 4 h at room temperature under Ar. The suspension was filtered and the filtrate was evaporated. Flash chromatography (*n*-pentane/Et_2O 4:1) of the crude product thus obtained afforded complex **15** (109 mg, 37%) as a violet solid. ^{1}H NMR (CD_2Cl_2, 200 MHz): $\delta = 19.16$ (s, 1H), 7.86 (br, 2H), 7.50–7.25 (m, 1H), 7.41 (t, 1H, $J = 7.1$ Hz), 7.12 (t, 2H, $J = 7.8$ Hz), 6.80 (m, 1H), 6.30 (m, 2H), 4.83 (t, 2H, $J = 4.6$ Hz), 4.35 (t, 2H, $J = 4.6$ Hz), 2.45–2.05 (m, 3H), 2.34 (s, 3H), 1.92 (s, 6H), 1.90–1.50 (m, 15H), 1.45–1.05 (m, 15H), 0.94 (s, 6H), 0.09 (s, 6H); ^{31}P NMR (CD_2Cl_2, 81 MHz): $\delta =$ 35.4; IR: $\tilde{\nu} = 3167$, 3129, 3100, 3055, 2925, 2850, 1907, 1609, 1471, 1462, 1445, 1250, 1232, 1118, 1074, 894, 847, 829, 779 cm^{-1}; MS (ESI): *m*/*z*: 851 $[M -$ Cl$]^+$; elemental analysis calcd for $C_{45}H_{71}Cl_2N_2OPRuSi$ (887.10): C 60.93, H 8.07, N 3.16; found C 61.11, H 8.13, N 3.11.

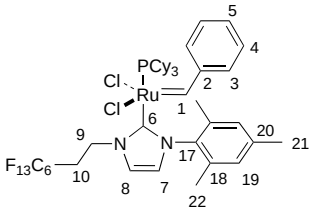

Complex 16: Imidazolium salt **7e** (300 mg, 0.45 mmol), KO*t*Bu (51 mg, 0.46 mmol) and complex **1** (281 mg, 0.34 mmol) were stirred in toluene (20 mL) for 1.5 h at room temperature. The suspension was filtered, the filtrate was evaporated and the residue purified by flash chromatography (*n*-pentane/Et_2O 4:1 → CH_2Cl_2) to afford complex **16** (155 mg, 42%) as a violet solid. ^{1}H NMR (CD_2Cl_2, 300 MHz): $\delta = 19.21$ (s, 1H, 1-H), 7.82 (br, 2H, 3-H), 7.44 (t, 1H, $J = 7.3$ Hz, 5-H), 7.26 (s, 1H, 9-H), 7.14 (t, 2H, $J =$ 7.7 Hz, 4-H), 6.87 (d, 1H, $J = 1.9$ Hz, 8-H), 6.31 (br, 2H, 19-H), 5.04 (t, 2H, $J = 7.0$ Hz, 9-H), 3.18 (tt, 2H, $J = 19.5$, 7.0 Hz, 7-H), 2.35 (s, 3H, 21-H), 2.30–2.15 (m, 3H), 1.91 (s, 6H, 22-H), 1.80–1.60 (m, 15H), 1.50–1.10 (m, 15H); ^{31}P NMR (CD_2Cl_2, 81 MHz): $\delta = 32.3$; ^{19}F NMR (CD_2Cl_2, 282 MHz): $\delta = -81.1$ (t, 3F, $^3J_{FF} = 8.7$ Hz, F-16), -113.1 (br, 2F), -121.9 (br, 2F), -122.9 (br, 2F), -123.5 (br, 2F), -126.3 (br, 2F); IR: $\tilde{\nu} = 3170$, 3130, 3099, 3076, 3060, 2928, 2852, 1611, 1588, 1571, 1490, 1448, 1348, 1239, 1194, 1145, 1122, 1078, 1025, 895, 848, 743, 689 cm^{-1}; MS (ESI): *m*/*z*: 1039.6 $[M -$ Cl$]^+$; elemental analysis calcd for $C_{45}H_{56}Cl_2F_{13}N_2PRu$ (1074.87): C 50.28, H 5.25, N 2.61; found C 50.21, H 5.34, N 2.56.

Complex 17: A solution of KO*t*Bu (117 mg, 1.04 mmol) in THF (20 mL) was slowly added at ambient temperature under Ar to a solution of 2-*tert*-butoxy-1,3-bis(2,6-di-isopropylphenyl)-4,5-dihydro-imidazole (437 mg, 1.02 mmol) in THF (20 mL). The suspension was stirred at room temperature for 2 h and added to a solution of complex **1** (545 mg, 0.66 mmol) in toluene (40 mL). The reaction mixture was stirred for 30 min at 80 °C and the solvent evaporated in vacuo. Washing of the residue at room temperature with anhydrous methanol (4 × 10 mL) and drying in vacuo afforded product **17** (412 mg, 67%) as a violet-brownish solid. ^{1}H NMR (CD_2Cl_2, 200 MHz): $\delta = 19.44$ (s, 1H, 1-H), 7.92 (br d, 2H, $J = 6.8$ Hz, 3-H), 7.45–7.25 (m, 5H), 7.03 (t, 2H, $J = 7.9$ Hz, 4-H), 6.75 (s, 2H, 12-H), 4.13 (m, 2H, 12′-H), 4.06–3.87 (m, 4H, 7-H, 7′-H), 3.52 (sept., 2H, $J = 6.9$ Hz, 12-H), 2.15–2.00 (m, 3H), 1.50–1.40 (m, 9H), 1.48 (d, 6H, $J = 6.5$ Hz), 1.36 (d, 6H, $J =$ 6.6 Hz), 1.35–1.30 (m, 6H), 1.21 (d, 6H, $J = 6.9$ Hz), 1.11 (d, 6H, $J =$ 6.9 Hz), 1.00–0.90 (m, 15H); ^{31}P NMR (CD_2Cl_2, 81 MHz): $\delta = 27.1$; IR: $\tilde{\nu} = 3063$, 2963, 2924, 2848, 1901, 1587, 1462, 1445, 1406, 1382, 1265, 1234, 1172, 1005, 894, 847, 803, 758, 736, 687 cm^{-1}; MS (ESI): *m*/*z*: calcd for $C_{52}H_{77}Cl_2N_2PRu$: 933.15; found: 897.6 $[M - Cl]^+$; HR-MS: calcd: 897.4551; found: 897.4574.

Enyne metathesis reactions—Representative procedure. Synthesis of 3-(2-methyl-propenyl)-1-(toluene-4-sulfonyl)-2,5-dihydro-1*H*-pyrrole (45a, R = H): A solution of enyne **44a** (R = H, 55.5 mg, 0.2 mmol) and complex **2** (8.4 mg, 0.01 mmol) in toluene (20 mL) was stirred at 80 °C for 30 min. The solvent was evaporated and the residue purified by flash chromatography (hexanes/ethyl acetate 4:1) affording product **45a** as a colorless solid (49.4 mg, 89%). ^{1}H NMR (300 MHz, $CDCl_3$): $\delta = 7.70$ (AA′XX′, 2H), 7.28 (AA′XX′, 2H), 5.58 (s, 1H), 5.35 (s, 1H), 4.24–4.17 (m, 2H), 4.15–4.08 (m, 2H), 2.37 (s, 3H), 1.75 (s, 3H), 1.72 (s, 3H); ^{13}C NMR (75.5 MHz, $CDCl_3$): $\delta = 143.4$, 137.9, 136.3, 134.2, 129.7, 127.4, 120.9, 118.0, 56.2, 54.5, 27.2, 21.5, 19.9; IR (KBr): $\tilde{\nu} = 3120$, 3065, 2965, 2914, 2843, 1639, 1624, 1595, 1492, 1477, 1452, 1343, 1324, 1302, 1291, 1211, 1162, 1122, 1096, 1069, 1016, 997, 853, 835, 817, 738, 708, 670, 603, 551, 526 cm^{-1}; MS (EI): *m*/*z* (%): 277 (27) $[M]^+$, 155 (9), 122 (100), 106 (32), 91 (51), 80 (54), 65 (18), 55 (12), 41 (14); HR-MS (EI): calcd: $C_{15}H_{19}NO_2S$: 277.1137, found: 277.1132.

2,2-Diphenyl-3-vinyl-2,5-dihydro-furan (29a, R = H): ^{1}H NMR ($CDCl_3$, 300 MHz): $\delta = 7.35–7.22$ (m, 10H), 6.23 (ddm, 1H, $J = 17.8$, 11.2 Hz), 6.16 (m, 1H), 5.31 (dm, 1H, $J = 17.8$ Hz), 5.09 (dm, 1H, $J = 11.2$ Hz), 4.77 (s, 2H); ^{13}C NMR ($CDCl_3$, 75 MHz): $\delta = 143.7$, 143.3, 129.8, 127.9, 127.9, 127.4, 124.9, 117.5, 94.5, 73.2; IR (film): $\tilde{\nu} = 3084$, 2977, 2945, 2838, 1642, 1597, 1490, 1446, 1064, 990, 912, 758, 699 cm^{-1}; MS (EI): *m*/*z* (%): 248 (38) $[M]^+$, 230 (9), 205 (16), 171 (100), 143 (13), 128 (24), 115 (19), 105 (44), 91 (30), 77 (32); HR-MS: calcd: 248.1201; found: 248.1206.

4-Methyl-2,2-diphenyl-3-vinyl-2,5-dihydro-furan (29b, R = Me): ^{1}H NMR ($CDCl_3$, 200 MHz): $\delta = 7.50–7.15$ (m, 10H), 6.31 (dd, 1H, $J = 17.8$, 11.5 Hz), 5.14 (d, 1H, $J = 11.5$ Hz), 5.02 (d, 1H, $J = 17.8$ Hz), 4.68 (s, 2H), 1.90 (s, 3H); ^{13}C NMR ($CDCl_3$, 50 MHz): $\delta = 143.9$, 135.4, 135.2, 128.8, 128.0, 127.7, 127.3, 117.9, 96.1, 77.1, 11.1; IR (film): $\tilde{\nu} = 3085$, 3058, 3024, 2980, 2936, 2913, 2855, 2827, 1653, 1600, 1490, 1446, 1378, 1057, 991, 907, 759, 700 cm^{-1}; MS (EI): *m*/*z* (%): 262 (22) $[M]^+$, 247 (5), 229 (8), 205 (14), 185 (100), 165 (10), 129 (11), 115 (12), 105 (45), 91 (23), 77 (35); HR-MS: calcd: 262.1358; found: 262.1360.

2-Methyl-2-phenyl-3-vinyl-2,5-dihydro-furan (31a, R = H): ^{1}H NMR (CD_2Cl_2, 300 MHz): $\delta = 7.40–7.24$ (m, 5H), 6.22 (ddm, 1H, $J = 17.9$, 11.2 Hz), 6.00 (m, 1H), 5.07 (dm, 1H, $J = 17.9$ Hz), 5.00 (dm, 1H, $J =$ 11.2 Hz), 4.73 (s, 2H), 1.76 (s, 3H); ^{13}C NMR (CD_2Cl_2, 75 MHz): $\delta =$ 145.3, 145.1, 129.5, 128.5, 127.7, 126.5, 124.9, 116.9, 90.0, 73.5, 24.5; IR (film): $\tilde{\nu} = 3087$, 2977, 2838, 1645, 1593, 1493, 1446, 1069, 989, 912, 764, 698 cm^{-1}; MS (EI): *m*/*z* (%): 186 (10) $[M]^+$, 171 (100), 153 (8), 143 (35), 128 (31), 115 (17), 109 (14), 105 (7), 91 (7), 77 (20), 51 (13), 43 (18).

2,4-Dimethyl-2-phenyl-3-vinyl-2,5-dihydro-furan (31b, R = Me): ^{1}H NMR ($CDCl_3$, 200 MHz): $\delta = 7.55–7.25$ (m, 5H), 6.39 (ddm, 1H, $J = 17.4$, 11.5 Hz), 5.11 (dm, 1H, $J = 11.5$ Hz), 5.05 (dm, 1H, $J = 17.4$ Hz),

4.76 – 4.74 (m, 2H), 1.93 (s, 3H), 1.89 (s, 3H); ^{13}C NMR ($CDCl_3$, 50 MHz): δ = 145.7, 136.8, 134.4, 128.4, 127.8, 127.5, 126.6, 116.1, 91.6, 77.4, 24.4, 10.7; IR (film): $\tilde{\nu}$ = 3088, 3059, 3026, 2978, 2933, 2856, 2827, 1658, 1601, 1494, 1446, 1037, 990, 909, 764, 698 cm^{-1}; MS (EI): *m*/*z* (%): 200 (5) $[M]^+$, 185 (100), 167 (6), 157 (9), 143 (30), 129 (22), 115 (12), 105 (18), 91 (13), 77 (26), 43 (45); HR-MS: calcd: 200.1201; found: 200.1205.

2-Methyl-2-phenyl-3-(2-methyl-prop-2-enyl)-2,5-dihydro-furan (33): ^{1}H NMR ($CDCl_3$, 200 MHz): δ = 7.55 – 7.10 (m, 5H), 5.71 (s, 1H), 5.32 (m, 1H), 4.85 (s, 2H), 1.80 (s, 3H), 1.77 (s, 3H), 1.67 (s, 3H); ^{13}C NMR ($CDCl_3$, 50 MHz): δ = 145.3, 143.1, 139.4, 128.0, 127.0, 125.7, 120.8, 116.4, 91.2, 74.0, 26.9, 25.0, 20.1; IR (film): $\tilde{\nu}$ = 3086, 2974, 2929, 2837, 1649, 1601, 1493, 1446, 1378, 1071, 763, 698 cm^{-1}; MS (EI): *m*/*z* (%): 214 (18) $[M]^+$, 199 (100), 181 (18), 171 (28), 157 (10), 157 (10), 143 (20), 129 (18), 115 (13), 105 (35), 91 (24), 79 (82), 51 (15), 43 (36); HR-MS: calcd: 214.1358, found: 214.1366.

3-Isopropenyl-2-methyl-2-phenyl-2,5-dihydro-furan (35a, R = Me): ^{1}H NMR (CD_2Cl_2, 300 MHz): δ = 7.50 – 7.38 (m, 2H), 7.35 – 7.25 (m, 3H), 6.05 (s, 1H), 4.82 (s, 1H), 4.72 (s, 2H), 4.54 (s, 1H), 1.91 (s, 3H), 1.83 (s, 3H); ^{13}C NMR (CD_2Cl_2, 75 MHz): δ = 146.7, 145.3, 136.0, 128.4, 127.6, 126.7, 124.9, 115.2, 90.3, 73.1, 24.4, 22.5; IR (film): $\tilde{\nu}$ = 3087, 3060, 2976, 2836, 1635, 1495, 1447, 1371, 1251, 1237, 1073, 1044, 895, 764, 698 cm^{-1}; MS (EI): *m*/*z* (%): 200 (66) $[M]^+$, 185 (100), 167 (20), 157 (81), 143 (20), 142 (30), 141 (18), 129 (27), 128 (19), 115 (16), 105 (27), 79 (39), 77 (29), 51 (11), 43 (28); HR-MS: calcd: 200.1201, found: 200.1202.

2-Methyl-2-phenyl-3-(1-phenyl-vinyl)-2,5-dihydro-furan (35b, R = Ph): ^{1}H NMR (CD_2Cl_2, 300 MHz): δ = 7.48 – 7.45 (m, 2H), 7.37 – 7.26 (m, 8H), 5.80 (t, *J* = 1.9 Hz, 1H), 5.03 (s, 1H), 4.81 (s, 1H), 4.75 (d, *J* = 1.9 Hz, 2H), 1.87 (s, 3H); ^{13}C NMR (CD_2Cl_2, 75.5 MHz): δ = 146.2, 145.2, 142.9, 142.5, 128.5, 128.4, 128.3, 128.0, 127.8, 127.7, 126.6, 116.6, 90.8, 73.4, 24.6; IR (neat): $\tilde{\nu}$ = 3083, 3057, 3027, 2978, 2983, 2840, 1720, 1659, 1599, 1573, 1493, 1445, 1370, 1336, 1235, 1183, 1129, 1096, 1071, 1054, 1027, 953, 905, 865, 819, 777, 765, 699, 629, 594, 562, 530 cm^{-1}; MS (EI): *m*/*z* (%): 262 (71) $[M]^+$, 247 (100), 229 (25), 219 (69), 204 (20), 185 (13), 171 (13), 155 (4), 141 (89), 128 (15), 115 (44), 103 (77), 91 (49), 77 (52), 63 (8), 51 (19), 43 (32); HR-MS (EI): calcd for $C_{19}H_{18}O$: 262.1358, found: 262.1357.

2,2′,2′,2′-Tetramethyl-2,5,2′,5′-tetrahydro-[3,3′]bifuranyl (37): ^{1}H NMR (CD_2Cl_2, 300 MHz): δ = 5.76 (s, 2H), 4.57 (s, 4H), 1.39 (s, 12H); ^{13}C NMR (CD_2Cl_2, 75 MHz): δ = 139.3, 122.6, 88.8, 72.3, 27.4; IR (KBr): $\tilde{\nu}$ = 3091, 1970, 1836, 1638, 1459, 1364, 1272, 1195, 1145, 1074, 806, 761 cm^{-1}; MS (EI): *m*/*z* (%): 194 (27) $[M]^+$, 179 (100), 135 (31), 121 (26), 109 (11), 107 (13), 93 (26), 91 (20), 78 (29), 55 (11), 43 (84); HR-MS: calcd: 194.1307, found: 194.1308.

4-Isopropenyl-3,6-dihydro-2*H*-pyran (39): ^{1}H NMR (300 MHz, CD_2Cl_2): δ = 5.82 (m, 1H), 4.99 (m, 1H), 4.91 (m, 1H), 4.22 (m, 2H), 3.79 (t, *J* = 5.5 Hz, 2H), 2.28 (m, 2H), 1.90 (m, 3H); ^{13}C NMR (75 MHz, CD_2Cl_2): δ = 142.8, 134.7, 123.2, 110.7, 66.0, 64.7, 26.1, 20.0; MS (EI): *m*/*z* (%): 125 (5), 124 (67) $[M]^+$, 123 (5), 110 (7), 109 (100), 95 (14), 93 (7), 91 (12), 83 (26), 81 (45), 79 (37), 77 (26), 67 (46), 65 (14), 55 (41), 53 (32), 52 (6), 51 (16), 43 (13), 41 (35), 39 (44), 29 (13), 27 (27). Due to the lability of this diene, the product was subjected to a Diels – Alder reaction with dimethyl acetylenedicarboxylate (toluene, 4 h, reflux) to afford the corresponding cycloadduct (76% over both steps) which gave the following spectroscopic and analytical data: m.p. 140 – 142 °C; ^{1}H NMR (300 MHz, CD_2Cl_2): δ = 4.00 (dd, *J* = 10.2, 4.2 Hz, 2H), 3.73 (s, 3H), 3.72 (s, 3H), 3.33 – 3.19 (m, 2H), 3.07 (t, *J* = 10.4 Hz, 1H), 2.99 (d, *J* = 7.2 Hz, 1H), 2.86 (m, 1H), 2.58 (m, 1H), 2.07 (m, 1H), 1.69 (s, 3H); ^{13}C NMR (75 MHz, CD_2Cl_2): δ = 168.4, 167.8, 133.9, 132.4, 126.0, 120.8, 72.4, 69.5, 52.4, 52.3, 41.7, 33.8, 30.3, 17.5; IR: $\tilde{\nu}$ = 2996, 2970, 2951, 2906, 2871, 2849, 1730, 1714, 1655, 1440, 1406, 1376, 1280, 1271, 1243, 1227, 1188, 1154, 1124, 1102, 1083, 1068, 1024, 968, 911, 898, 839, 790, 759, 666 cm^{-1}; MS (EI): *m*/*z* (%): 267 (3), 266 (22) $[M]^+$, 235 (27), 234 (39), 219 (35), 205 (12), 204 (34), 203 (12), 191 (12), 190 (29), 189 (10), 178 (13), 177 (100), 175 (10), 146 (12), 145 (39), 133 (10), 118 (16), 117 (22), 115 (19), 105 (12), 103 (11), 91 (25), 77 (13), 59 (22), 45 (12); HR-MS (EI): calcd for $C_{14}H_{18}O_5$: 266.1154, found: 266.1153; elemental analysis calcd for $C_{14}H_{18}O_5$ (266.29): C 63.15, H 6.81; found C 63.22, H 6.77.

3-Isopropenyl-1-(toluene-4-sulfonyl)-2,5-dihydro-1*H*-pyrrole (41): ^{1}H NMR ($CDCl_3$, 300 MHz): δ = 7.71 (AA′XX′, 2H), 7.29 (AA′XX′, 2H), 6.32 (dd, *J* = 17.7, 10.8 Hz, 1H), 5.56 (s, 1H), 4.95 (s, 1H), 4.74 (s, 1H), 4.24 – 4.15 (m, 4H), 2.39 (s, 3H), 1.82 (s, 3H); ^{13}C NMR ($CDCl_3$, 75.5 MHz): δ = 143.3, 139.2, 136.5, 134.1, 129.8, 127.4, 120.6, 114.5, 55.5, 54.3, 21.5, 19.9; IR (KBr): $\tilde{\nu}$ = 3088, 2958, 2921, 2840, 1641, 1606, 1596, 1492, 1475, 1457, 1344, 1305, 1290, 1253, 1164, 1100, 1071, 1016, 987, 895, 833, 816, 709, 672, 619, 575, 549 cm^{-1}; MS (EI): *m*/*z* (%): 263 (46) $[M]^+$, 222 (9), 155 (16), 108 (100), 91 (53), 81 (40), 65 (20), 53 (8), 41 (17); HR-MS (EI): calcd for $C_{14}H_{17}NO_2S$: 263.0980, found: 263.0974.

3-Styryl-1-(toluene-4-sulfonyl)-2,5-dihydro-1*H*-pyrrole (43a, R = H, *E*:*Z* = 3.4:1): ^{1}H NMR (300 MHz, CD_2Cl_2): δ = [*E*-isomer] 7.75 (AA′XX′, 2H), 7.41 – 7.22 (m, 7H), 6.81 (dd, *J* = 16.5, 0.6 Hz, 1H), 6.37 (d, *J* = 16.4 Hz, 1H), 5.71 (m, 1H), 4.32 (m, 2H), 4.21 (m, 2H), 2.42 (s, 3H); δ = [*Z*-isomer] 7.56 (AA′XX′, 2H), 7.41 – 7.22 (m, 5H), 7.12 (m, 2H), 6.59 (d, *J* = 12.0 Hz, 1H), 6.14 (m, 1H), 5.63 (m, 1H), 4.04 (m, 2H), 3.70 (m, 2H), 2.44 (s, 3H); ^{13}C NMR (75 MHz, CD_2Cl_2): δ = [*E*-isomer] 144.1, 137.6, 136.8, 134.3, 131.6, 130.2, 129.0, 128.4, 127.8, 126.8, 124.0, 121.8, 55.6, 54.1, 21.6; δ = [*Z*-isomer, where resolved] 144.1, 137.8, 136.4, 134.0, 132.3, 130.1, 128.9, 128.3, 127.9, 126.0, 123.7, 55.3, 54.6, 21.6; IR: $\tilde{\nu}$ = 3026, 2922, 2899, 2832, 1596, 1492, 1461, 1450, 1398, 1379, 1345, 1302, 1291, 1263, 1208, 1183, 1163, 1106, 1072, 1016, 985, 960, 828, 812, 792, 752, 722, 708, 693, 670, 603, 572, 546, 529 cm^{-1}; MS (EI): *m*/*z* (%): 326 (8), 325 (31) $[M]^+$, 171 (13), 170 (100), 169 (66), 168 (55), 167 (12), 155 (12), 154 (12), 153 (53), 143 (44), 142 (11), 141 (29), 128 (35), 115 (31), 92 (27), 91 (90), 65 (35), 42 (12), 39 (13); HR-MS (EI): calcd for $C_{19}H_{19}NO_2S$: 325.1137, found: 325.1131; elemental analysis calcd for $C_{19}H_{19}NO_2S$ (325.43): C 70.12; H 5.89; N 4.30; found C 69.94; H 6.11; N 4.06.

3-(1-Methyl-2-phenyl-vinyl)-1-(toluene-4-sulfonyl)-2,5-dihydro-1*H*-pyrrole (43b, R = Me, *E*:*Z* = 2:1): ^{1}H NMR (300 MHz, CD_2Cl_2): δ = [*E*-isomer] 7.75 (AA′XX′, 2H), 7.44 – 7.20 (m, 7H), 6.32 (s, 1H), 5.73 (m, 1H), 4.37 (m, 2H), 4.22 (m, 2H), 2.43 (s, 3H), 1.99 (d, *J* = 0.9 Hz, 3H); δ = [*Z*-isomer] 7.54 (AA′XX′, 2H), 7.44 – 7.20 (m, 5H), 7.06 (m, 2H), 6.48 (s, 1H), 5.58 (m, 1H), 4.11 – 4.03 (m, 2H), 3.75 – 3.71 (m, 2H), 2.45 (s, 3H), 1.94 (d, 3H, *J* = 1.4 Hz); ^{13}C NMR (75 MHz, CD_2Cl_2): δ = [*E*-isomer] δ = 144.1, 140.9, 137.5, 134.2, 130.7, 130.2, 129.6, 128.5, 127.8, 127.3, 123.6, 121.0, 55.9, 54.8, 21.6, 15.3; δ = [*Z*-isomer] 144.0, 139.0, 138.2, 133.9, 131.0, 130.0, 129.0, 128.9, 128.3, 127.3, 125.8, 122.6, 55.5, 54.9, 24.3, 19.3; IR: $\tilde{\nu}$ = 3056, 3025, 2950, 2919, 2856, 1597, 1492, 1473, 1444, 1399, 1345, 1305, 1290, 1165, 1099, 1070, 1018, 991, 919, 834, 816, 792, 754, 706, 668, 605, 575, 550 cm^{-1}; MS (EI): *m*/*z* (%): 340 (16), 339 (66) $[M]^+$, 185 (14), 184 (100), 183 (55), 182 (56), 169 (16), 168 (47), 167 (73), 157 (43), 156 (34), 155 (34), 143 (11), 142 (21), 141 (22), 129 (23), 128 (15), 115 (28), 106 (11), 92 (10), 91 (84), 65 (18), 42 (16); HR-MS (EI): calcd for $C_{20}H_{21}NO_2S$: 339.1293, found: 339.1292; elemental analysis calcd for $C_{20}H_{21}NO_2S$ (339.46): C 70.77, H 6.24, N 4.13; found: C 70.58, H 6.30, N 4.06.

3-Methyl-2-[1-(toluene-4-sulfonyl)-2,5-dihydro-1*H*-pyrrol-3-yl]-but-2-enoic acid methyl ester (45b, R = CO$_2$Me): ^{1}H NMR (300 MHz, CD_2Cl_2): δ = 7.71 (AA′XX′, 2H), 7.35 (AA′XX′, 2H), 5.38 (m, 1H), 4.16 (m, 2H), 4.12 (m, 2H), 3.60 (s, 3H), 2.43 (s, 3H), 2.01 (s, 3H), 1.69 (s, 3H); ^{13}C NMR (75 MHz, CD_2Cl_2): δ = 167.3, 149.7, 144.1, 135.9, 134.5, 130.1, 127.8, 124.3, 122.5, 57.1, 55.6, 51.7, 23.6, 22.7, 21.6; IR: $\tilde{\nu}$ = 3065, 3028, 2989, 2950, 2918, 2867, 1717, 1620, 1598, 1494, 1434, 1399, 1372, 1346, 1306, 1285, 1223, 1163, 1093, 1017, 1007, 985, 921, 885, 816, 777, 760, 709, 669, 603, 549 cm^{-1}; MS (EI): *m*/*z* (%): 336 (7), 335 (35) $[M]^+$, 180 (24), 148 (27), 121 (11), 120 (100), 93 (15), 91 (39), 77 (11), 65 (12); HR-MS (EI): calcd for $C_{17}H_{21}NO_4S$: 335.1191, found: 335.1194; elemental analysis calcd for $C_{17}H_{21}NO_4S$ (335.42): C 60.87, H 6.31, N 4.18; found C 60.94, H 6.26, N 4.10.

5-Isopropenyl-1-(toluene-4-sulfonyl)-1,2,3,6-tetrahydro-pyridine (47): ^{1}H NMR ($CDCl_3$, 300 MHz): δ = 7.67 (AA′XX′, 2H), 7.29 (AA′XX′, 2H), 5.87 – 5.81 (m, 1H), 4.85 (s, 1H), 4.82 (s, 1H), 3.77 – 3.72 (m, 2H), 3.13 (d, *J* = 5.8 Hz, 2H), 2.39 (s, 3H), 2.33 – 2.26 (m, 2H), 1.82 (m, 3H); ^{13}C NMR ($CDCl_3$, 75.5 MHz): δ = 143.5, 140.5, 133.5, 133.0, 129.6, 127.6, 122.3, 110.4, 45.0, 42.3, 25.5, 21.5, 20.5; IR (KBr): $\tilde{\nu}$ = 3061, 2961, 2925, 2865, 1716, 1642, 1597, 1569, 1494, 1458, 1382, 1364, 1341, 1306, 1241, 1165, 1101, 1018, 970, 899, 816, 770, 744, 658, 564, 548 cm^{-1}; MS (EI): *m*/*z* (%): 277 (9) $[M]^+$, 262 (6), 236 (2), 155 (15), 121 (68), 106 (21), 95 (61), 79 (100), 65 (24), 55 (14), 41 (21).

3-Isopropenyl-1-(toluene-4-sulfonyl)-2,5,6,7-tetrahydro-1*H*-azepine (49): ^{1}H NMR ($CDCl_3$, 300 MHz): δ = 7.64 (AA′XX′, 2H), 7.24 (AA′XX′, 2H), 5.87 (t, *J* = 6.2 Hz, 1H), 5.11 (s, 1H), 4.93 (s, 1H), 4.06 (s, 2H), 3.39 (t, *J* = 6.1 Hz, 2H), 2.39 (s, 3H), 2.26 – 2.18 (m, 2H), 1.83 (d, *J* = 0.8 Hz, 3H), 1.75 – 1.66 (m, 2H); ^{13}C NMR ($CDCl_3$, 75.5 MHz): δ = 142.9, 142.3, 139.1, 136.4, 129.7, 129.4, 127.1, 111.7, 50.5, 46.9, 26.4, 26.3, 21.4, 21.3; IR (KBr): $\tilde{\nu}$ = 3047, 2936, 2852, 1698, 1641, 1599, 1494, 1455, 1337, 1305, 1266, 1240,

0947-6539/01/0715-3250 $ 17.50+.50/0 *Chem. Eur. J.* **2001**, *7*, No. 15

1160, 1094, 1044, 1018, 928, 906, 881, 816, 737, 708, 657, 596, 548 cm^{-1}; MS (EI): *m/z* (%): 291 (28) $[M]^+$, 276 (5), 263 (1), 248 (12), 224 (14), 184 (11), 155 (40), 136 (100), 120 (20), 107 (26), 91 (73), 79 (25), 65 (22), 55 (10), 41 (28); HR-MS (EI): calcd for $C_{16}H_{21}NO_2S$: 291.1293, found: 291.1295.

1-(4-{1-[1-(Toluene-4-sulfonyl)-2,5-dihydro-1*H*-pyrrol-3-yl]-vinyl}-phenyl)-ethanone (51): ^1H NMR (CD_2Cl_2, 300 MHz): δ = 7.90 (AA′XX′, 2H), 7.74 (AA′XX′, 2H), 7.37 (AA′XX′, 2H), 7.31 (AA′XX′, 2H), 5.47–5.43 (m, 1H), 5.24 (s, 1H), 5.16 (s, 1H), 4.38–4.32 (m, 2H), 4.23–4.15 (m, 2H), 2.57 (s, 3H), 2.35 (s, 3H); ^{13}C NMR (CD_2Cl_2, 75.5 MHz): δ = 197.7, 145.1, 144.2, 142.6, 138.1, 137.0, 134.3, 130.2, 128.8, 128.5, 127.8, 124.8, 117.0, 56.0, 55.1, 26.8, 21.6; IR (neat): $\tilde{\nu}$ = 3062, 2922, 2854, 1682, 1649, 1604, 1560, 1494, 1427, 1402, 1345, 1306, 1267, 1162, 1097, 1066, 1015, 958, 909, 883, 815, 709, 668, 620, 591, 549 cm^{-1}; MS (EI): *m/z* (%): 367 (58) $[M]^+$, 222 (19); 212 (50), 196 (18), 170 (74), 155 (43), 91 (100), 65 (25), 43 (87).

3-Isopropenyl-cyclopent-3-ene-1,1-dicarboxylic acid diethyl ester (53): ^1H NMR (300 MHz, CD_2Cl_2): δ = 5.61 (m, 1H), 4.95 (s, 1H), 4.91 (d, J = 0.6 Hz, 1H), 4.17 (q, J = 7.1 Hz, 4H), 3.14 (m, 2H), 3.08 (m, 2H), 1.91 (s, 3H), 1.24 (t, J = 7.1 Hz, 6H); ^{13}C NMR (75 MHz, CD_2Cl_2): δ = 172.3, 141.8, 139.5, 124.3, 113.3, 61.9, 59.2, 41.4, 40.8, 20.5, 14.2; IR: $\tilde{\nu}$ = 3089, 3062, 2981, 2939, 2907, 2868, 1733, 1634, 1603, 1445, 1385, 1367, 1250, 1183, 1161, 1119, 1068, 1016, 987, 888, 820, 709 cm^{-1}; MS (EI): *m/z* (%): 253 (4), 252 (22) $[M]^+$, 207 (10), 179 (31), 178 (100), 150 (13), 133 (20), 119 (21), 106 (18), 105 (48), 91 (40), 79 (14), 77 (13), 29 (53), 27 (12); HR-MS (EI): calcd for $C_{14}H_{20}O_4$: 252.1362, found: 252.1367; elemental analysis calcd for $C_{14}H_{20}O_4$ (252.31): C 66.65, H 7.99; found C 66.78, H 8.07.

2-(1,3-Dihydro-benzo[*c*]oxepin-5-yl)-acrylic acid methyl ester (55): ^1H NMR (300 MHz, CD_2Cl_2): δ = 7.33–7.27 (m, 3H), 7.16 (m, 1H), 6.35 (d, J = 1.6 Hz, 1H), 6.17 (t, J = 5.1 Hz, 1H), 5.85 (d, J = 1.7 Hz, 1H), 4.55 (s, 2H), 4.17 (d, J = 5.1 Hz, 2H), 3.60 (s, 3H); ^{13}C NMR (75 MHz, CD_2Cl_2): δ = 167.1, 143.1, 140.8, 139.0, 138.5, 130.8, 129.2, 128.2, 128.1, 128.0, 127.9, 70.4, 67.1, 52.2; IR: $\tilde{\nu}$ = 3099, 3060, 3022, 2994, 2951, 2916, 2856, 1723, 1618, 1572, 1488, 1448, 1436, 1379, 1361, 1320, 1303, 1271, 1235, 1210, 1149, 1113, 1098, 1057, 1041, 985, 953, 898, 881, 860, 830, 812, 775, 761, 735, 714, 610, 594 cm^{-1}; MS (EI): *m/z* (%): 231 (5), 230 (35) $[M]^+$, 202 (20), 197 (11), 187 (20), 186 (10), 171 (14), 170 (26), 169 (34), 155 (12), 153 (31), 144 (13), 143 (96), 142 (53), 141 (100), 139 (16), 129 (26), 128 (81), 127 (18), 115 (67), 91 (12), 89 (12), 77 (10), 63 (14), 51 (10), 39 (12); HR-MS (EI): calcd for $C_{14}H_{14}O_3$: 230.0943, found: 230.0944; elemental analysis calcd for $C_{14}H_{14}O_3$ (230.26): C 73.03, H 6.13; found C 73.15, H 6.06.

Crystal Data for 9–11 and 13–15, 18: Single crystals suitable for X-ray analysis were mounted on glass fibers using perfluoropolyether. X-ray intensities were measured at 100 K using $Mo_{K\alpha}$ (λ = 0.71073 Å) radiation, employing either a Nonius KappaCCD system and a rotating anode generator (**11**, **14**, **15**, **18**) or a Bruker AXS Smart system equipped with a sealed tube (**9**, **10**, **13**). One hemisphere of data was collected in case of the SMART system and a two-fold redundancy was aimed for in case of the KappaCCD system. Integrated intensities including Lorentz and polarization corrections were obtained using the SAINT (Bruker AXS) [SAINT Ver. 6.01, Bruker AXS Inc. Madison, Wisconsin, USA, 1999] and Denzo-SMN (Nonius)[44] programs respectively. For further crystal and data collection details see Table 7.

All crystal structures were solved using the SHELXS-97 [G. M. Sheldrick, Program for the solution of crystal structures, University of Göttingen, Germany, **1997**] program, either by direct methods (**9**, **13**) or interpretation of the Patterson function. The function $w(F_o^2 - F_c^2)^2$ was minimized using full matrix least-squares refinement implemented in the program SHELXL-97 [G. M. Sheldrick, Program for the refinement of crystal structures, University of Göttingen, Germany, **1997**]. Atomic positions and anisotropic displacement parameters were included for all non-hydrogen atoms, with the exception of **9** (cyclohexane solvent and disordered phenyl substituent) and **10** (all carbon atoms) where isotropic displacement parameters were employed. Hydrogen atoms were placed at calculated positions and were allowed to ride on the corresponding parent atom with isotropic displacement parameters 1.2 times (1.5 times for methyl) of the parent atom. A summary of the results is given in Table 7 ($R = \Sigma||F_o| - |F_c||/\Sigma\ |F_o|$, $wR2 = \{\Sigma[w(F_o^2 - F_c^2)^2]/\Sigma\ [w(F_o^2)^2]\}^{1/2}$, $GoF = \{\Sigma[w(F_o^2 - F_c^2)^2]/(n-p)\}^{1/2}$, with n equals number of reflections and p equals number of parameters).

Crystallographic data (excluding structure factors) for the structures reported in this paper have been deposited with the Cambridge Crystallo-

Table 7. Crystal data and details of the structure determination for **9**–**11**, **13**–**15** and **18**.

	9	**10**	**11**	**13**	**14**	**15**	**18**
formula	$C_{46}H_{61}Cl_4N_2PRu$	$C_{57}H_{87}Cl_2N_2PRu$	$C_{48}H_{60}Cl_2N_3PRu$	$C_{35}H_{55}Cl_2N_2PRu$	$C_{34}H_{53}Cl_2N_2PRu$	$C_{47.5}H_{77}Cl_2N_2OPRuSi$	$C_{36}H_{68}Cl_2P_2Ru$
color	brown	red-brown	black	yellow	brown	dark red	yellow
M_w [g mol^{-1}]	915.81	1003.23	881.93	706.75	692.72	947.15	734.81
crystal system	monoclinic	monoclinic	monoclinic	monoclinic	monoclinic	triclinic	triclinic
space group	*Cc* (no. 9)	$P2_1/n$ (no. 14)	$P2_1/c$ (no. 14)	$P2_1/c$ (no. 14)	$C2/c$ (no. 15)	$P\bar{1}$ (no. 2)	$P\bar{1}$, (no. 2)
a [Å]	12.1730(6)	28.3376(9)	18.8745(12)	18.413(2)	40.4367(8)	9.7413(2)	9.705(10)
b [Å]	7.9632(18)	14.3007(6)	10.9962(8)	9.9087(11)	9.7598(2)	15.5112(3)	10.121(13)
c [Å]	9.7070(5)	29.2250(12)	20.9943(12)	18.759(2)	19.0674(6)	17.8850(3)	10.719(8)
α [°]						65.7930(10)	114.13(4)
β [°]	97.418(2)	107.416(2)	102.700(3)	91.275(4)	117.701(2)	84.8880(10)	108.29(3)
γ [°]						80.4940(10)	91.48(5)
V [Å^3]	4448.3(4)	11300.4(8)	4250.7(5)	3421.7(6)	6662.5(3)	2430.25(8)	897.8(16)
Z	4	8	4	4	8	2	1
ρ_{calcd} [Mg m^{-3}]	1.367	1.179	1.378	1.372	1.381	1.294	1.359
μ [mm^{-1}]	0.663	0.436	0.570	0.688	0.705	0.939	0.699
F(000) [e$^-$]	1912	4288	1848	1488	2912	1001	392
crystal size [mm]	0.26 × 0.16 × 0.16	0.28 × 0.24 × 0.21	0.16 × 0.08 × 0.03	0.54 × 0.40 × 0.02	0.19 × 0.09 × 0.09	0.30 × 0.13 × 0.03	0.25 × 0.10 × 0.08
θ range for data collection	1.77 to 33.17°	2.04 to 24.00°	2.05 to 27.47	2.17 to 27.49	3.41 to 27.82°	3.43 to 33.20°	2.23 to 27.56°
refls. collected	24700	36240	20661	28511	25497	29616	8293
indep. refls.	10683	15256	8670	7758	7831	18425	4131
R_{int}	0.0529	0.2060	0.1780	0.1562	0.0779	0.0732	0.0855
obs. refls. with $I > 2\sigma(I)$	8175	5291	2847	5524	5907	10943	3369
compl. to θ	33.17°/97.6%	24.00°/85.9%	27.47°/88.9%	27.49°/98.6%	27.82°/99.1%	27.50°/99.6%	27.56°/99.7%
data/parameters	10683/490	15256/599	8670/471	7758/373	7831/382	18425/514	4131/187
GoF	1.018	0.916	0.881	1.051	1.002	0.984	1.122
R [$I > 2\sigma(I)$]	0.0544	0.0984	0.0780	0.0710	0.0418	0.0603	0.0507
*wR*2 (all data)	0.1191	0.2880	0.2429	0.2258	0.1059	0.1263	0.1572
flack parameter	0.07(3)	–	–	–	–	–	–
max. diff. peak/hole [e Å^{-3}]	1.485/−0.800	0.824/−0.886	0.915/−1.342	2.077/−5.077	0.812/−0.461	0.755/−0.897	1.034/−2.062

graphic Data Centre as supplementary publication no. CCDC – 154931 (**10**), CCDC-154932 (**18**), CCDC-154933 (**11**), CCDC-154934 (**9**), CCDC-154935 (**13**), CCDC-154936 (**15**) and CCDC-156357 (**14**). Copies of the data can be obtained free of charge on application to CCDC, 12 Union Road, Cambridge CB2 1EZ, UK (fax: (+44) 1223-336-033; e-mail: deposit @ccdc.cam.ac.uk).

Acknowledgement

Generous financial support by the Deutsche Forschungsgemeinschaft (Leibniz award to A.F.) and the Fonds der Chemischen Industrie (Kekulé stipends to L.A. and F.S.) is acknowledged with gratitude. We thank Dr. K. Angermund for carrying out AM1 calculations for compounds **28** and **29**.

[1] a) S. T. Nguyen, R. H. Grubbs, J. W. Ziller, *J. Am. Chem. Soc.* **1993**, *115*, 9858 – 9859; b) S. T. Nguyen, L. K. Johnson, R. H. Grubbs, J. W. Ziller, *J. Am. Chem. Soc.* **1992**, *114*, 3974 – 3975; c) P. Schwab, R. H. Grubbs, J. W. Ziller, *J. Am. Chem. Soc.* **1996**, *118*, 100 – 110.

[2] Recent reviews: a) A. Fürstner, *Angew. Chem.* **2000**, *112*, 3140 – 3172; *Angew. Chem. Int. Ed.* **2000**, *39*, 3012 – 3043; b) R. H. Grubbs, S. Chang, *Tetrahedron* **1998**, *54*, 4413 – 4450; c) A. Fürstner, *Top. Organomet. Chem.* **1998**, *1*, 37 – 72; d) S. K. Armstrong, *J. Chem. Soc. Perkin Trans. 1* **1998**, 371 – 388; e) M. Schuster, S. Blechert, *Angew. Chem.* **1997**, *109*, 2124 – 2144; *Angew. Chem. Int. Ed. Engl.* **1997**, *36*, 2037 – 2056; f) A. Fürstner, *Top. Catal.* **1997**, *4*, 285 – 299; g) K. J. Ivin, J. C. Mol, *Olefin Metathesis and Metathesis Polymerization*, Academic Press, San Diego, **1997**.

[3] a) J. Wolf, W. Stüer, C. Grünwald, H. Werner, P. Schwab, M. Schulz, *Angew. Chem.* **1998**, *110*, 1165 – 1167; *Angew. Chem. Int. Ed.* **1998**, *37*, 1124 – 1126; b) T. R. Belderrain, R. H. Grubbs, *Organometallics* **1997**, *16*, 4001 – 4003; c) T. E. Wilhelm, T. R. Belderrain, S. N. Brown, R. H. Grubbs, *Organometallics* **1997**, *16*, 3867 – 3869.

[4] a) E. L. Dias, S. T. Nguyen, R. H. Grubbs, *J. Am. Chem. Soc.* **1997**, *119*, 3887 – 3897; b) O. M. Aagaard, R. J. Meier, F. Buda, *J. Am. Chem. Soc.* **1998**, *120*, 7174 – 7182; c) C. Hinderling, C. Adlhart, P. Chen, *Angew. Chem.* **1998**, *110*, 2831 – 2835; *Angew. Chem. Int. Ed.* **1998**, *37*, 2685 – 2689.

[5] a) A. Fürstner, M. Picquet, C. Bruneau, P. H. Dixneuf, *Chem. Commun.* **1998**, 1315 – 1316; b) A. Fürstner, M. Liebl, C. W. Lehmann, M. Picquet, R. Kunz, C. Bruneau, D. Touchard, P. H. Dixneuf, *Chem. Eur. J.* **2000**, *6*, 1847 – 1857; c) A. Demonceau, A. W. Stumpf, E. Saive, A. F. Noels, *Macromolecules* **1997**, *30*, 3127 – 3136; d) A. Hafner, A. Mühlebach, P. A. van der Schaaf, *Angew. Chem.* **1997**, *109*, 2213 – 2216; *Angew. Chem. Int. Ed. Engl.* **1997**, *36*, 2121 – 2124; e) A. Fürstner, L. Ackermann, *Chem. Commun.* **1999**, 95 – 96; f) S. M. Hansen, M. A. O. Volland, F. Rominger, F. Eisenträger, P. Hofmann, *Angew. Chem.* **1999**, *111*, 1360 – 1364; *Angew. Chem. Int. Ed.* **1999**, *38*, 1273 – 1276; g) S. M. Hansen, F. Rominger, M. Metz, P. Hofmann, *Chem. Eur. J.* **1999**, *5*, 557 – 566; h) H. Katayama, F. Ozawa, *Organometallics* **1998**, *17*, 5190 – 5196; i) A. Fürstner, A. F. Hill, M. Liebl, J. D. E. T. Winton-Ely, *Chem. Commun.* **1999**, 601 – 602; j) M. Ahmed, A. G. M. Barrett, D. C. Braddock, S. M. Cramp, P. A. Procopiou, *Tetrahedron Lett.* **1999**, *40*, 8657 – 8662.

[6] a) S. Chang, L. Jones, C. Wang, L. M. Henling, R. H. Grubbs, *Organometallics* **1998**, *17*, 3460 – 3465; b) E. L. Dias, R. H. Grubbs, *Organometallics* **1998**, *17*, 2758 – 2767; c) M. S. Sanford, L. M. Henling, R. H. Grubbs, *Organometallics* **1998**, *17*, 5384 – 5389; d) J. S. Kingsbury, J. P. A. Harrity, P. J. Bonitatebus, A. H. Hoveyda, *J. Am. Chem. Soc.* **1999**, *121*, 791 – 799.

[7] a) J. Huang, E. D. Stevens, S. P. Nolan, J. L. Pedersen, *J. Am. Chem. Soc.* **1999**, *121*, 2674 – 2678; b) J. Huang, H.-J. Schanz, E. D. Stevens, S. P. Nolan, *Organometallics* **1999**, *18*, 5375 – 5380.

[8] a) M. Scholl, T. M. Trnka, J. P. Morgan, R. H. Grubbs, *Tetrahedron Lett.* **1999**, *40*, 2247 – 2250; b) M. Scholl, S. Ding, C. W. Lee, R. H. Grubbs, *Org. Lett.* **1999**, *1*, 953 – 956.

[9] a) L. Ackermann, A. Fürstner, T. Weskamp, F. J. Kohl, W. A. Herrmann, *Tetrahedron Lett.* **1999**, *40*, 4787 – 4790; b) T. Weskamp, F. J. Kohl, W. Hieringer, D. Gleich, W. A. Herrmann, *Angew. Chem.* **1999**, *111*, 2573 – 2576; *Angew. Chem. Int. Ed.* **1999**, *38*, 2416 – 2419; c) U. Frenzel, T. Weskamp, F. J. Kohl, W. C. Schattenmann, O. Nuyken, W. A. Herrmann, *J. Organomet. Chem.* **1999**, *586*, 263 – 265.

[10] For reviews see: a) W. A. Herrmann, C. Köcher, *Angew. Chem.* **1997**, *109*, 2256 – 2282; *Angew. Chem. Int. Ed. Engl.* **1997**, *36*, 2162 – 2187; b) D. Bourissou, O. Guerret, F. P. Gabbai, G. Bertrand, *Chem. Rev.* **2000**, *100*, 39 – 91; c) A. J. Arduengo, *Acc. Chem. Res.* **1999**, *32*, 913 – 921; d) for an investigation of the thermochemistry of Ru^{II}–NHC as compared to Ru^{II}–PR_3 bonds see: J. Huang, H.-J. Schanz, E. D. Stevens, S. P. Nolan, *Organometallics* **1999**, *18*, 2370 – 2375.

[11] A. Fürstner, O. R. Thiel, L. Ackermann, H.-J. Schanz, S. P. Nolan, *J. Org. Chem.* **2000**, *65*, 2204 – 2207.

[12] A. K. Chatterjee, J. P. Morgan, M. Scholl, R. H. Grubbs, *J. Am. Chem. Soc.* **2000**, *122*, 3783 – 3784.

[13] a) L. Ackermann, D. El Tom, A. Fürstner, *Tetrahedron* **2000**, *56*, 2195 – 2202; b) A. Fürstner, O. R. Thiel, N. Kindler, B. Bartkowska, *J. Org. Chem.* **2000**, *65*, 7990 – 7995; c) A. Fürstner, O. R. Thiel, G. Blanda, *Org. Lett.* **2000**, *2*, 3731 – 3734; d) A. Fürstner, O. R. Thiel, L. Ackermann, *Org. Lett.* **2001**, *3*, 449 – 451.

[14] a) J. Limanto, M. L. Snapper, *J. Am. Chem. Soc.* **2000**, *122*, 8071 – 8072; b) I. Efremov, L. A. Paquette, *J. Am. Chem. Soc.* **2000**, *122*, 9324 – 9325; c) R. M. Garbaccio, S. J. Danishefsky, *Org. Lett.* **2000**, *2*, 3127 – 3129; d) L. Hyldtoft, R. Madsen, *J. Am. Chem. Soc.* **2000**, *122*, 8444 – 8452; e) J. C. J. Benningshof, R. H. Blaauw, A. E. van Ginkel, F. P. J. T. Rutjes, J. Fraanje, K. Goubitz, H. Schenk, H. Hiemstra, *Chem. Commun.* **2000**, 1465 – 1466; f) J. A. Smulik, S. T. Diver, *Org. Lett.* **2000**, *2*, 2271 – 2274; g) D. L. Wright, J. P. Schulte, M. A. Page, *Org. Lett.* **2000**, *2*, 1847 – 1850; h) C. W. Lee, R. H. Grubbs, *Org. Lett.* **2000**, *2*, 2145 – 2147; i) R. Stragies, U. Voigtmann, S. Blechert, *Tetrahedron Lett.* **2000**, *41*, 5465 – 5468; j) M. Ahmed, T. Arnauld, A. G. M. Barrett, D. C. Braddock, P. A. Procopiou, *Synlett* **2000**, 1007 – 1009; k) D. Bourgeois, J. Mahuteau, A. Pancrazi, S. P. Nolan, J. Prunet, *Synthesis* **2000**, 869 – 882; l) T. Itoh, K. Mitsukura, N. Ishida, K. Uneyama, *Org. Lett.* **2000**, *2*, 1431 – 1434; m) A. Briot, M. Bujard, V. Gouverneur, S. P. Nolan, C. Mioskowski, *Org. Lett.* **2000**, *2*, 1517 – 1519.

[15] A few structural variants of **2** and **3** have been reported, although all of them contain *identical* substituents on both N-atoms of the NHC ligand, cf. ref. [9] and the following: a) S. C. Schürer, S. Gessler, N. Buschmann, S. Blechert, *Angew. Chem.* **2000**, *112*, 4062 – 4065; *Angew. Chem. Int. Ed.* **2000**, *39*, 3898 – 3901; b) S. B. Garber, J. S. Kingsbury, B. L. Gray, A. H. Hoveyda, *J. Am. Chem. Soc.* **2000**, *122*, 8168 – 8179; c) L. Jafarpour, E. D. Stevens, S. P. Nolan, *J. Organomet. Chem.* **2000**, *606*, 49 – 54.

[16] A. J. Arduengo, R. Krafczyk, R. Schmutzler, H. A. Craig, J. R. Goerlich, W. J. Marshall, M. Unverzagt, *Tetrahedron* **1999**, *55*, 14523 – 14534.

[17] a) A. J. Arduengo, F. Davidson, H. V. R. Dias, J. R. Goerlich, D. Khasnis, W. J. Marshall, T. K. Prakasha, *J. Am. Chem. Soc.* **1997**, *119*, 12742 – 12749; b) A. J. Arduengo, H. V. R. Dias, R. L. Harlow, M. Kline, *J. Am. Chem. Soc.* **1992**, *114*, 5530 – 5534; c) A. J. Arduengo, R. L. Harlow, M. Kline, *J. Am. Chem. Soc.* **1991**, *113*, 361 – 363.

[18] W. A. Herrmann, C. Köcher, L. J. Gooßen, G. R. J. Artus, *Chem. Eur. J.* **1996**, *2*, 1627 – 1636.

[19] M. G. Gardiner, W. A. Herrmann, C. P. Reisinger, J. Schwarz, M. Spiegler *J. Organomet. Chem.* **1999**, *572*, 239 – 247.

[20] Alternatively catalytic amounts of *t*BuOK together with NaH can be used; this method has the advantage that the progress of carbene formation can be monitored by measuring the volume of H_2 formed, cf. ref. [17b]. If applicable, we prefer this method for its preparative convenience over an alternative procedure using NaH in liquid ammonia as the reaction medium, cf. ref. [18].

[21] a) D. Enders, K. Breuer, G. Raabe, J. Runsink, J. H. Teles, J.-P. Melder, K. Ebel, S. Brode, *Angew. Chem.* **1995**, *107*, 1119 – 1122; *Angew. Chem. Int. Ed. Engl.* **1995**, *34*, 1021 – 1023; b) for a detailed description of the reactivity of this carbene, including its reactions with olefins see: D. Enders, K. Breuer, J. Runsink, J. H. Teles, *Liebigs Ann.* **1996**, 2019 – 2028.

[22] L. Jafarpour, S. P. Nolan, *Organometallics* **2000**, *19*, 2055 – 2057.

[23] Complex **16** was designed to make such "second-generation" catalysts more soluble in supercritical CO_2; applications will be reported in a separate publication. For the first examples of RCM and ROMP in $scCO_2$ using the parent-complex **1** see: A. Fürstner, D. Koch, K.

  0947-6539/01/0715-3252 $ 17.50+.50/0

Langemann, W. Leitner, C. Six, *Angew. Chem.* **1997**, *109*, 2562–2565; *Angew. Chem. Int. Ed. Engl.* **1997**, *36*, 2466–2469.

[24] In solution, complex **11** gives rise to two sets of signals in the ^{1}H and ^{31}P NMR spectra; 2D EXSY confirm that this effect is due to rotamers around the Ru–NHC bond.

[25] R. O. Gould, A. M. Gray, P. Taylor, M. D. Walkinshaw, *J. Am. Chem. Soc.* **1985**, *107*, 5921–5927.

[26] T. Weskamp, W. C. Schattenmann, M. Spiegler, W. A. Herrmann, *Angew. Chem.* **1998**, *110*, 2631–2633; *Angew. Chem. Int. Ed.* **1998**, *37*, 2490–2493.

[27] C. W. Bielawski, R. H. Grubbs, *Angew. Chem.* **2000**, *112*, 3025–3028; *Angew. Chem. Int. Ed.* **2000**, *39*, 2903–2906.

[28] a) For a detailed discussion see ref. [11]. b) Note, that the decomposition of the catalyst also constitutes a potential source of ruthenium hydride species; although the decomposition pathways of the Grubbs catalyst **1** have been studied in some detail, the ruthenium species formed are not yet clear, cf.: M. Ulman, R. H. Grubbs, *J. Org. Chem.* **1999**, *64*, 7202–7207.

[29] C. Grünwald, O. Gevert, J. Wolf, P. Gonzalez-Herrero, H. Werner, *Organometallics* **1996**, *15*, 1960–1962.

[30] V. Rodriguez, S. Sabo-Etienne, B. Chaudret, J. Thoburn, S. Ulrich, H.-H. Limbach, J. Eckert, J.-C. Barthelat, K. Hussein, C. J. Marsden, *Inorg. Chem.* **1998**, *37*, 3475–3485.

[31] In this context the reader is referred to a recent report showing that the Grubbs catalyst **1** converts into $(PCy_3)_2RuCl_2H_2$ upon hydrogenation in CH_2Cl_2, cf. S. D. Drouin, G. P. A. Yap, D. E. Fogg, *Inorg. Chem.* **2000**, *39*, 5412–5414.

[32] According to our opinion some data reported in the literature are inadequate for an assessment of the reactivity of NHC containing catalysts. Complexes of this type were repeatedly applied to a single substrate such as diethyl diallylmalonate which reacts very smoothly even with the parent Grubbs carbene **1** and is therefore of limited value for probing the reactivity of more powerful catalysts.

[33] a) A. Fürstner, K. Langemann, *J. Org. Chem.* **1996**, *61*, 3942–3943; b) A. Fürstner, K. Langemann, *Synthesis* **1997**, 792–803.

[34] Monitoring of this transformation by GC and TLC shows that the formation of the cyclic monomer proceeds via an initial dimerization of substrate **25** at the monosubstituted alkene; the resulting dimer **26** is then converted into the cyclic monomer **27**. For a more detailed report on this observation see ref. [13d].

[35] Review: M. Mori, *Top. Organomet. Chem.* **1998**, *1*, 133–154.

[36] See ref. [14f, i] and the following for leading references: a) A. Kinoshita, N. Sakakibara, M. Mori, *J. Am. Chem. Soc.* **1997**, *119*, 12388–12389; b) R. Stragies, M. Schuster, S. Blechert, *Angew. Chem.* **1997**, *109*, 2628–2630; *Angew Chem. Int. Ed. Engl.* **1997**, *36*, 2518–2520; c) A. G. M. Barrett, S. P. D. Baugh, D. C. Braddock, K. Flack, V. C. Gibson, P. A. Procopiou, *Chem. Commun.* **1997**, 1375–1376; d) K. Hammer, K. Undheim, *Tetrahedron* **1997**, *53*, 10603–10614; e) A. Kinoshita, M. Mori, *Synlett* **1994**, 1020–1022; f) M. Mori, T. Kitamura, N. Sakakibara, Y. Sato, *Org. Lett.* **2000**, *2*, 543–545; g) M. Mori, N. Sakakibara, A. Kinoshita, *J. Org. Chem.* **1998**, *63*, 6082–6083; h) J. A. Smulik, S. T. Diver, *J. Org. Chem.* **2000**, *65*, 1788–1792 and references therein.

[37] While RCM is driven by the gain in entropy caused by the (gaseous) by-product (e.g. ethene) released during the course of the reaction, enyne metathesis is devoid of such an inherent driving force. Therefore most examples reported so far deal with the formation of five-membered rings which have the highest intrinsic bias for cyclization. For some successful applications to larger rings see ref. [36g].

[38] Compounds of this type undergo formal enyne metathesis reactions in the presence of $PtCl_2$ or electron deficient palladacycles as catalysts; for leading references see: a) N. Chatani, N. Furukawa, H. Sakurai, S. Murai, *Organometallics* **1996**, *15*, 901–903; b) B. M. Trost, M. K. Trost, *J. Am. Chem. Soc.* **1991**, *113*, 1850–1852; c) A. Fürstner, H. Szillat, B. Gabor, R. Mynott, *J. Am. Chem. Soc.* **1998**, *120*, 8305–8314; d) A. Fürstner, H. Szillat, F. Stelzer, *J. Am. Chem. Soc.* **2000**, *122*, 6785–6786.

[39] Leading references: a) M. T. Reetz, M. H. Becker, K. M. Kühling, A. Holzwarth, *Angew. Chem.* **1998**, *110*, 2792–2795; *Angew. Chem. Int. Ed.* **1998**, *37*, 2647–2650; b) A. Holzwarth, H.-W. Schmidt, W. F. Maier, *Angew. Chem.* **1998**, *110*, 2788–2792; *Angew. Chem. Int. Ed.* **1998**, *37*, 2644–2647; c) S. J. Taylor, J. P. Morken, *Science* **1998**, *280*, 267–270.

[40] Reviews on combinatorial methods in catalysis: a) B. Jandeleit, D. J. Schaefer, T. S. Powers, H. W. Turner, W. H. Weinberg, *Angew. Chem.* **1999**, *111*, 2648–2689; *Angew. Chem. Int. Ed.* **1999**, *38*, 2494–2532; b) M. T. Reetz, *Angew. Chem.* **2001**, *113*, 292–320; *Angew. Chem. Int. Ed.* **2001**, *40*, 284–310.

[41] M. T. Reetz, M. H. Becker, M. Liebl, A. Fürstner, *Angew. Chem.* **2000**, *112*, 1294–1298; *Angew. Chem. Int. Ed.* **2000**, *39*, 1236–1239.

[42] For preparative applications of this complex see: a) A. Fürstner, O. R. Thiel, *J. Org. Chem.* **2000**, *65*, 1738–1742; b) A. Fürstner, J. Grabowski, C. W. Lehmann, T. Kataoka, K. Nagai, *ChemBioChem* **2001**, *2*, 60–68; c) A. Fürstner, J. Grabowski, C. W. Lehmann, *J. Org. Chem.* **1999**, *64*, 8275–8280; d) A. Fürstner, K. Radkowski, *Chem. Commun.* **2001**, 671–672.

[43] AM1 calculations show that diene **28** is about 35 kcal mol^{-1} more stable than enyne **29**. This explains the exothermicity observed by the thermocamera. It is believed, however, that the much more dramatic evolution of heat in case of complexes **3** and **10** as compared to the other catalysts screened is partly due to the fact that the heating of the reaction mixture caused by the incipient reaction increases the reaction rate, thereby producing even more heat and a yet faster conversion. Such an "autocatalytic" effect is absent whenever the reaction rate is such that heat transfer to the surroundings occurs at similar rates as the progress of the reaction.

[44] Z. Otwinowski, W. Minor, *Methods Enzymol.* **1997**, *276*, 307–326.

Received: February 12, 2001 [F3067]